Magnetism in layered Ruthenates
Oberseminar WS 2007/08

Markus Braden

Universität zu Köln

17.12.2007

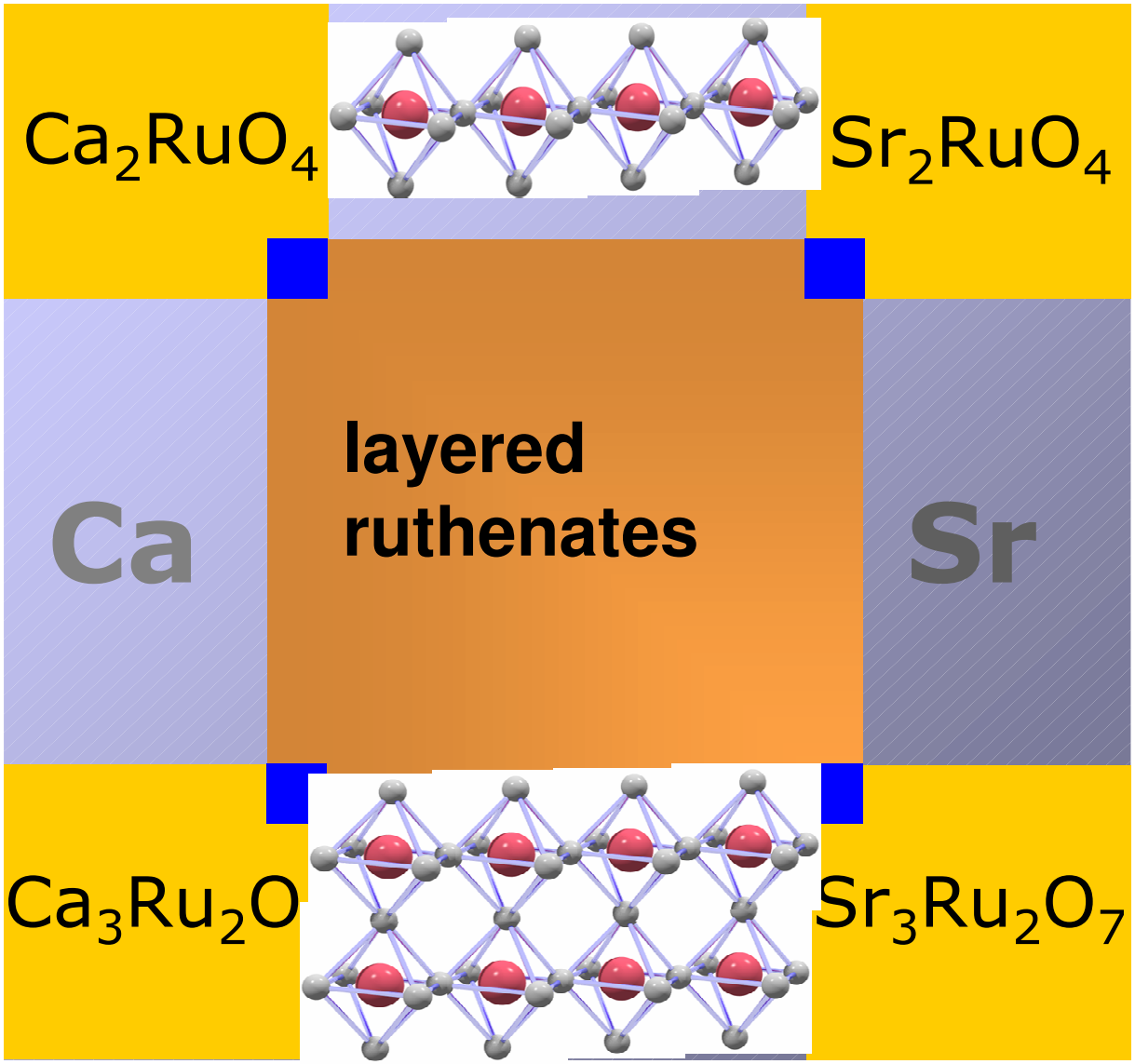

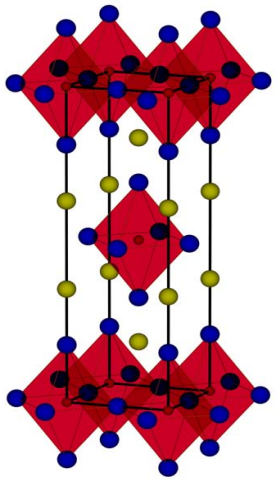

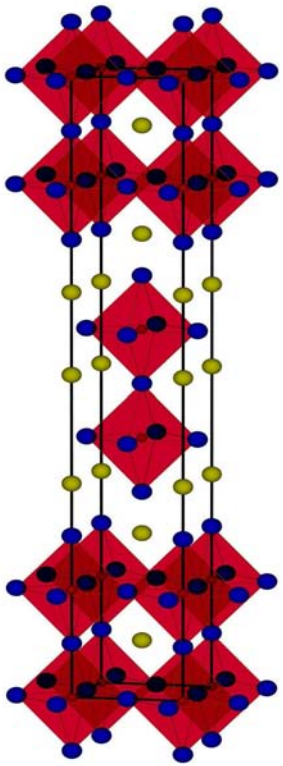

- **Ruddlesdon-Popper : n = 1,2, .. 3, 4, …**

Outline

1. superconducting Sr_2RuO_4
   - unconventional pairing
   - magnetic fluctuations
2. insulating Ca_2RuO_4
   - antiferromagnetism
   - role of orbital degrees of freedom
3. the phase diagram of $Ca_{2-x}Sr_xRuO_4$
   - strongly enhanced magnetic fluctuations
   - metamagnetism
4. double-layer materials : $Ca_{3-x}Sr_xRu_2O_7$
5. Conclusions

own work : collaboration with

P. Steffens, O. Schumann, O. Friedt, M. Kriener, J. Baier, T. Lorenz . . .
Y. Sidis, P. Bourges, A. Gukasov, . . .
S. Nakatsuji & Y. Maeno

superconductivity in Sr_2RuO_4

$La_{2-x}Ba_xCuO_4$

T_c~ 35 K

Sr_2RuO_4

T_c~ 1.5 K

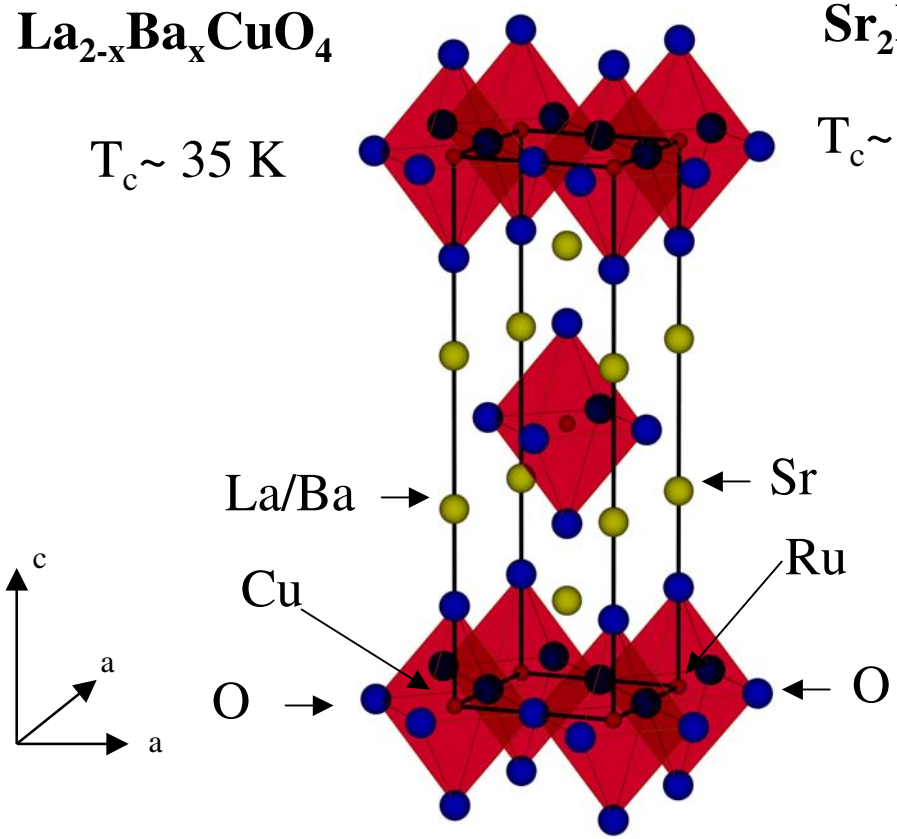

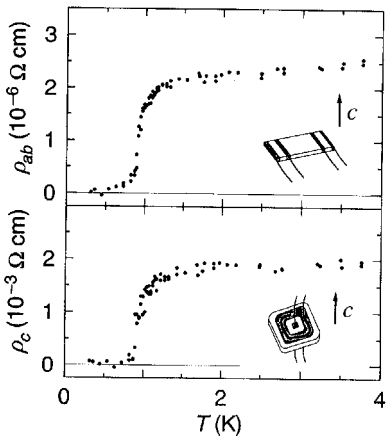

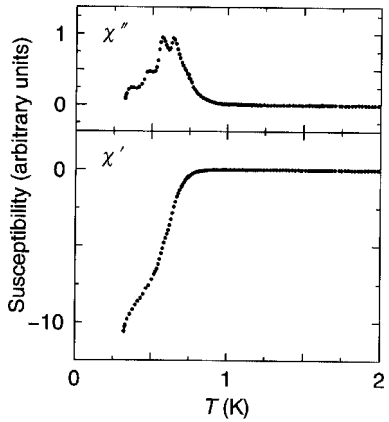

Y. Maeno *et al.*, Nature 1994

Normal-State properties

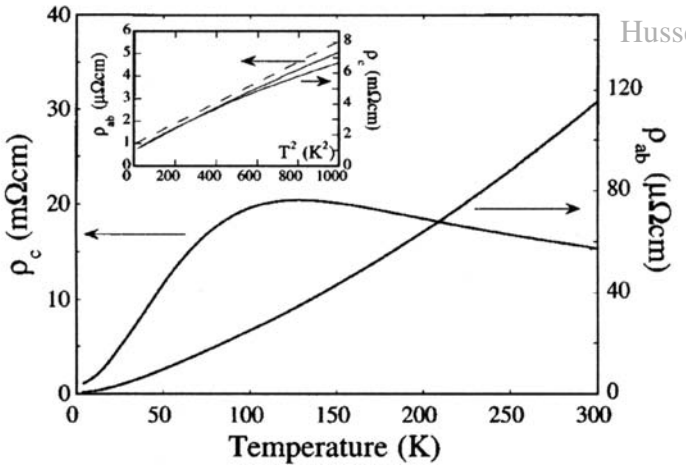

Hussey *et al.*, PRB 1998

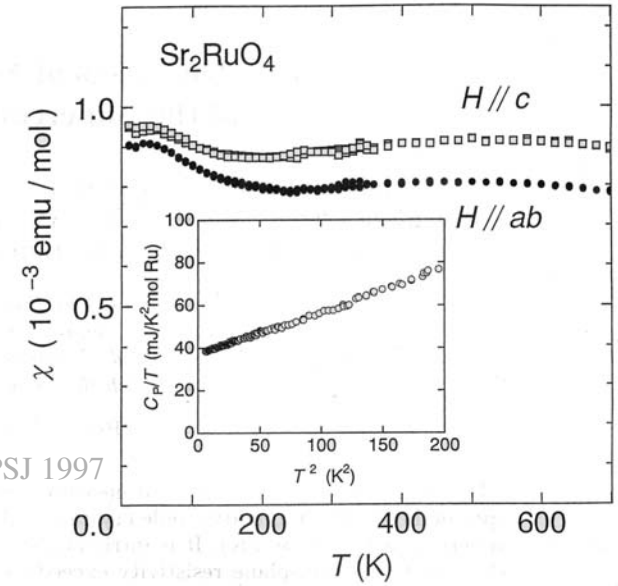

Maeno *et al.*, JPSJ 1997

Für T < 30 K:

- Anisotropic 3 dim. metal
- $\Gamma=\rho_c/\rho_{ab}$~450=const.

  at low temperatures
- $\rho(T)\sim T^2$ ➡ e^--e^--scattering

- Pauli-Paramagnetism S=1
- $c(T)=\gamma T+\beta T^3$ γ=40mJ/(mol K^2)
- Wilson-Ratio R_w=const.χ/γ=1.8

Fermi-liquid

impurity effect

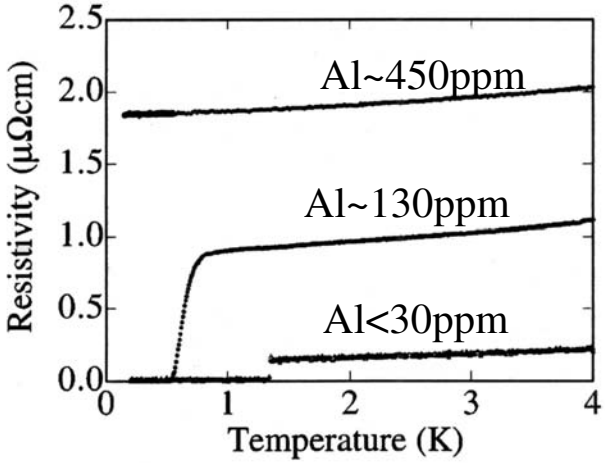

Mackenzie *et al.*, PRL 1998

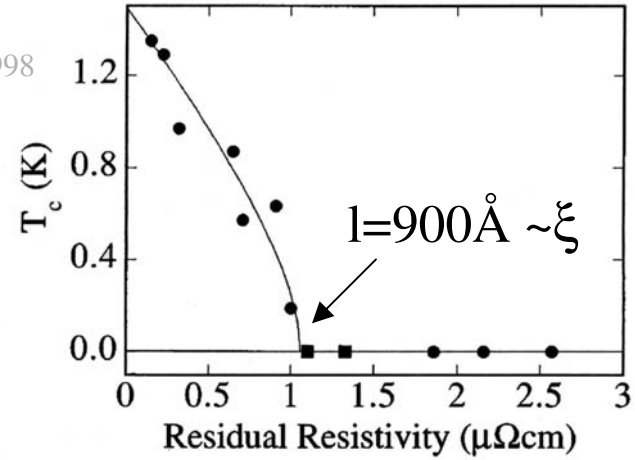

T_c extremely sensitive

- **non-magnetic impurities**
- **defects** Mao *et al.*, PRB 1999

s-wave pairing is unlikely

Verletzung der Zeit-Umkehr Invarianz

μ^+-Spin Relaxation:

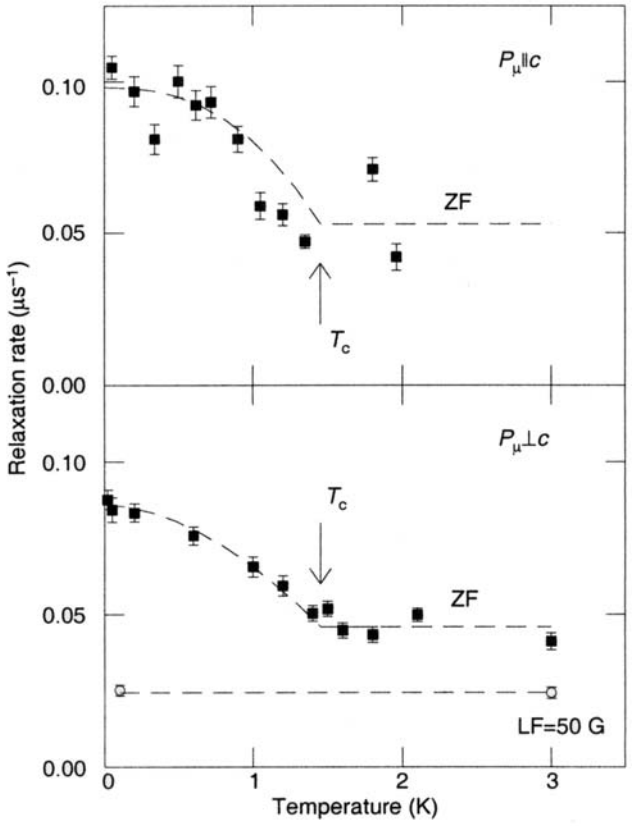

Luke *et al.*, Nature 1998

Spontanes internes **Magnetfeld** für $T<T_c$

Verletzung der T Invarianz

Evidenz für **p-Wellen** Symmetrie

$L_z=\pm 1$

^{17}O Knight Shift in Sr_2RuO_4

Spin-Susceptibility

Ishida *et al.*, Nature 1998

Singlet

↑↓

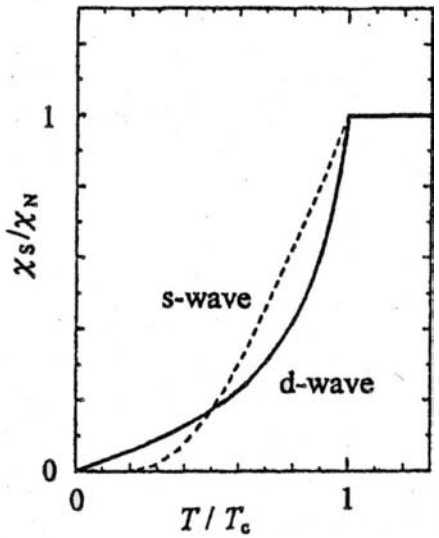

Triplet

↑↑

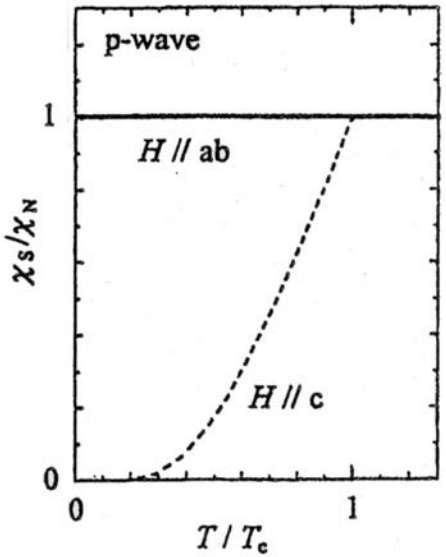

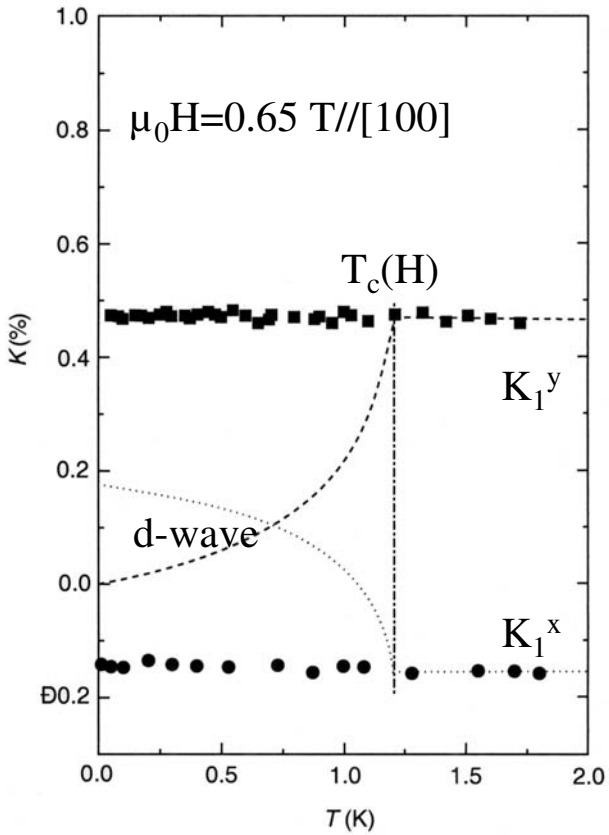

Spin-Susceptibility $K_S=K_N$

Spin-Triplet pairing

Spin-Triplet Superconductivity

Rice & Sigrist

Sr_2RuO_4 electronic analogue with ^3He

strong correlations

$SrRuO_3$ ferromagnet

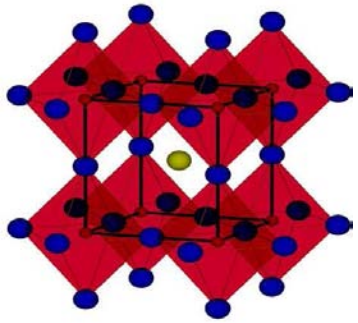

Sr_2RuO_4: spin-triplet superconductor with

p-wave symmetry

Cooper-Paar wavefunction: **$\Psi(2,1)=-\Psi(1,2)$** antisymmetric for Fermions

	Spin-part	**Orbital part**
Singlet	$S_z=0$ $\frac{1}{\sqrt{2}}\{\lvert\uparrow\downarrow\rangle-\lvert\downarrow\uparrow\rangle\}$	L=0,2,...(s,d,...wave)
S=0 $\uparrow\downarrow$	antisymmetric	symmetric,even parity
Triplet	$S_z=1$ $\lvert\uparrow\uparrow\rangle$	L=1,3,...(p,f,...wave)
S=1 $\uparrow\uparrow$	0 $\frac{1}{\sqrt{2}}\{\lvert\uparrow\downarrow\rangle+\lvert\downarrow\uparrow\rangle\}$	antisymmetric, odd parity
	-1 $\lvert\downarrow\downarrow\rangle$ symmetric	

Quantum interference devices

Odd-Parity Superconductivity in Sr_2RuO_4

K. D. Nelson,[1] Z. Q. Mao,[1*] Y. Maeno,[2,3] Y. Liu[1†]

Phase-sensitive measurements were made on Sr_2RuO_4 to establish unambiguously the odd-parity pairing in this material. The critical current of $Au_{0.5}In_{0.5}$-Sr_2RuO_4 superconducting quantum interference devices prepared on Sr_2RuO_4 single crystals was found to be a maximum for devices with junctions on the same side of the crystal and a minimum for devices with junctions on opposite sides, in the limit of zero magnetic flux; these findings indicate that the phase of the superconducting order parameter in Sr_2RuO_4 changes by π under inversion. This result verifies the odd-parity pairing symmetry and the formation of spin-triplet Cooper pairs in Sr_2RuO_4.

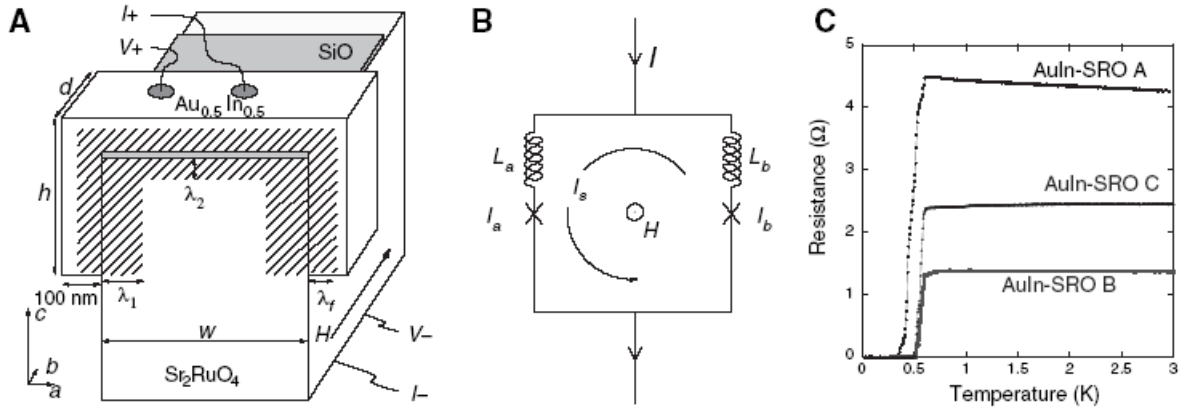

Fig. 1. (A) Schematic of $Au_{0.5}In_{0.5}$-Sr_2RuO_4 GLB SQUID with measurement leads. Both junctions in the SQUID are in-plane tunnel junctions to ensure $j_s \neq 0$. The side insulated by the SiO layer may cross the *ab* plane as depicted (samples A and B) or cross a third face perpendicular to the *ab* plane (sample C). The shaded area indicates the flux penetration at $T = 0$, $\lambda_1 \approx 3.7$ μm, and $\lambda_2 \approx 0.18$ μm. For sample C, the flux penetration is to a depth of λ_2 on all three sides. The value of λ_f is not known but may be slightly larger than that of pure In, 0.07 μm. For sample A, $w = 1.05$ mm, $h = 0.5$ mm, and $d = 0.33$ mm; for sample B, $w = 1.15$ mm, $h = 0.4$ mm (left) and 0.6 mm (right), and $d = 0.15$ mm; for sample C, $w = 0.68$ mm, $h = 0.3$ mm, and $d = 0.4$ mm. The SiO layer thickness is 150 nm. (B) Equivalent circuit of the SQUID. I_a and I_b are the current on the left and the right side of the SQUID loop, L_a and L_b are effective inductances, I is total current, and I_s is circulating current. (C) Sample resistance R as a function of T for three GLB SQUIDs. A smooth $R(T)$ across the T_c of Sr_2RuO_4 (around 1.4 K) indicates that $R(T)$ is dominated by the tunnel barrier.

Science 306, 1151 (2004)

High resolution polar Kerr effect

Jing Xia et al., PRL 97, 167002 (2006)

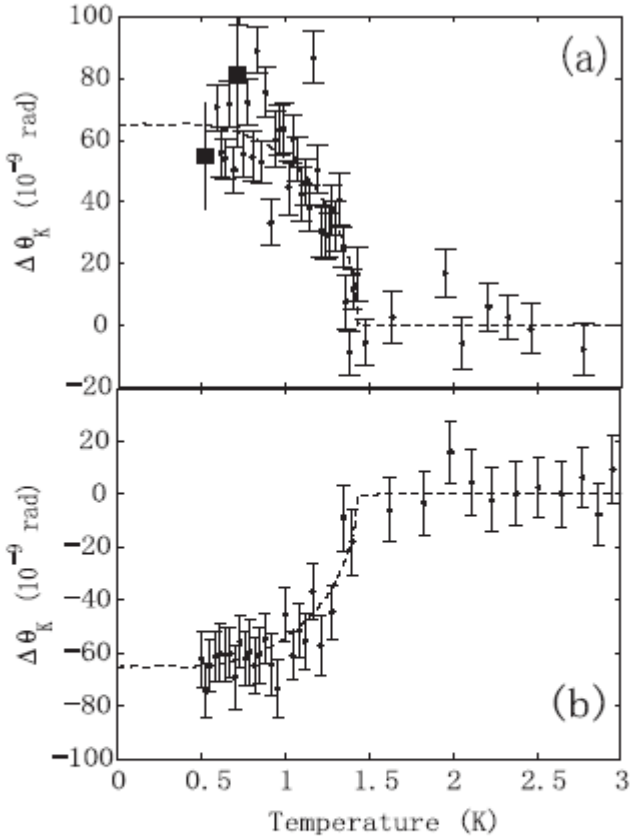

FIG. 3. Representative results of training the chirality with an applied field. (a) +93 Oe field cool, then zero-field warm-up (○). The two solid squares represent the last two points just before the field was turned off. (b) −47 Oe field cool, then zero-field warm-up (○). Dashed curves are fits to a BCS gap temperature dependence.

$$\vec{d} = \Delta_0 \cdot \hat{z} \cdot (k_x \pm i \cdot k_y) \cdot \begin{bmatrix} 0 \\ 0 \\ 1 \end{bmatrix}$$

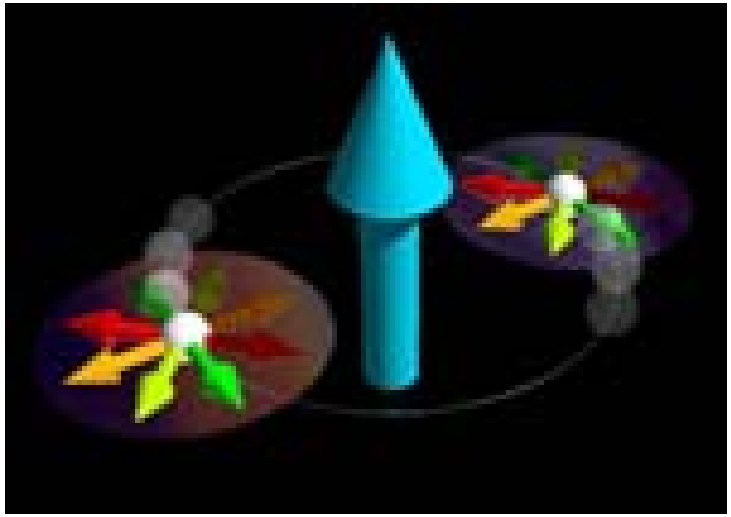

A.P. Mackenzie and Y. Maeno, Rev. Mod. Phys. **75**, 657 (2003).

Magnetism in Sr_2RuO_4 and inelastic neutron scattering

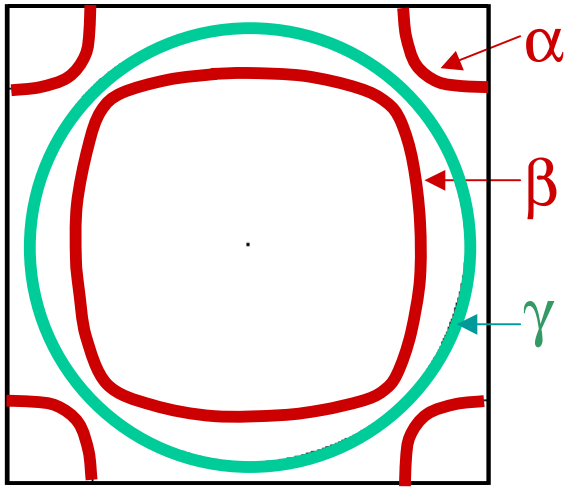

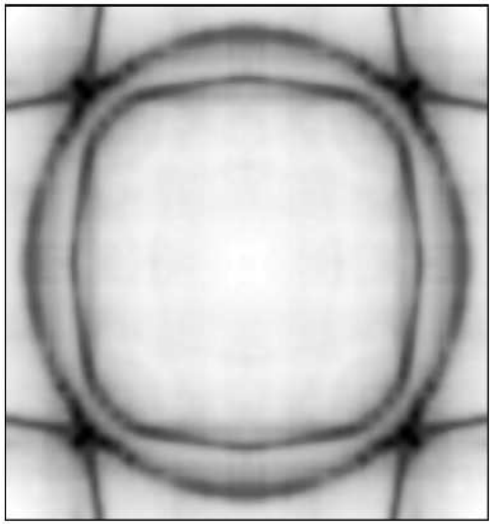

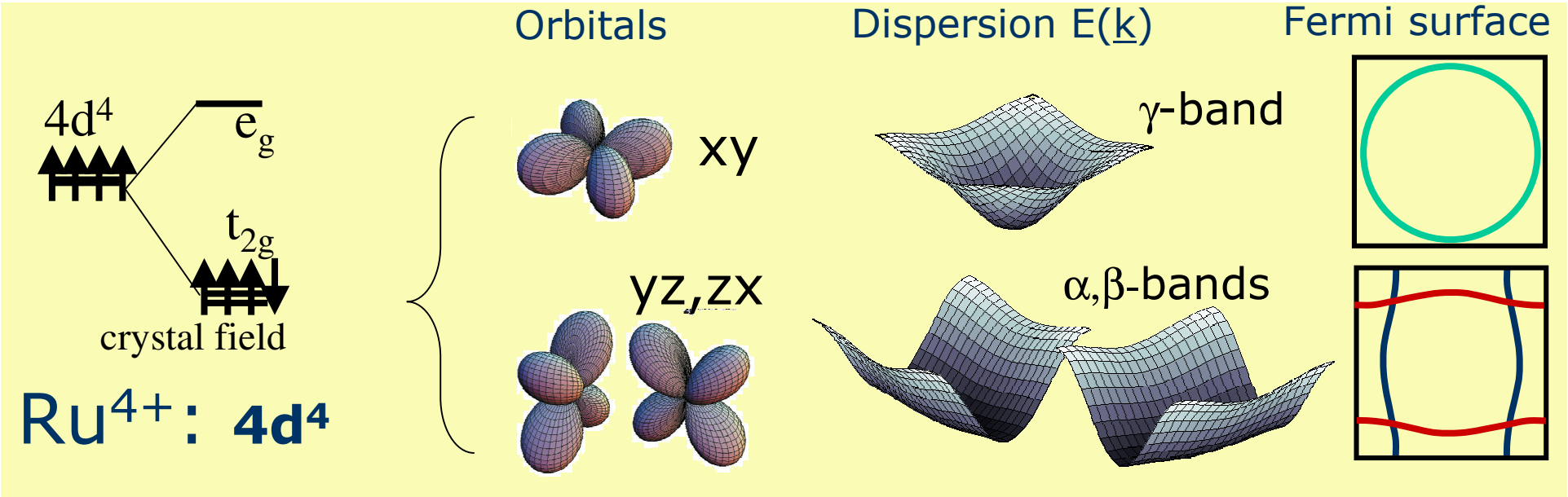

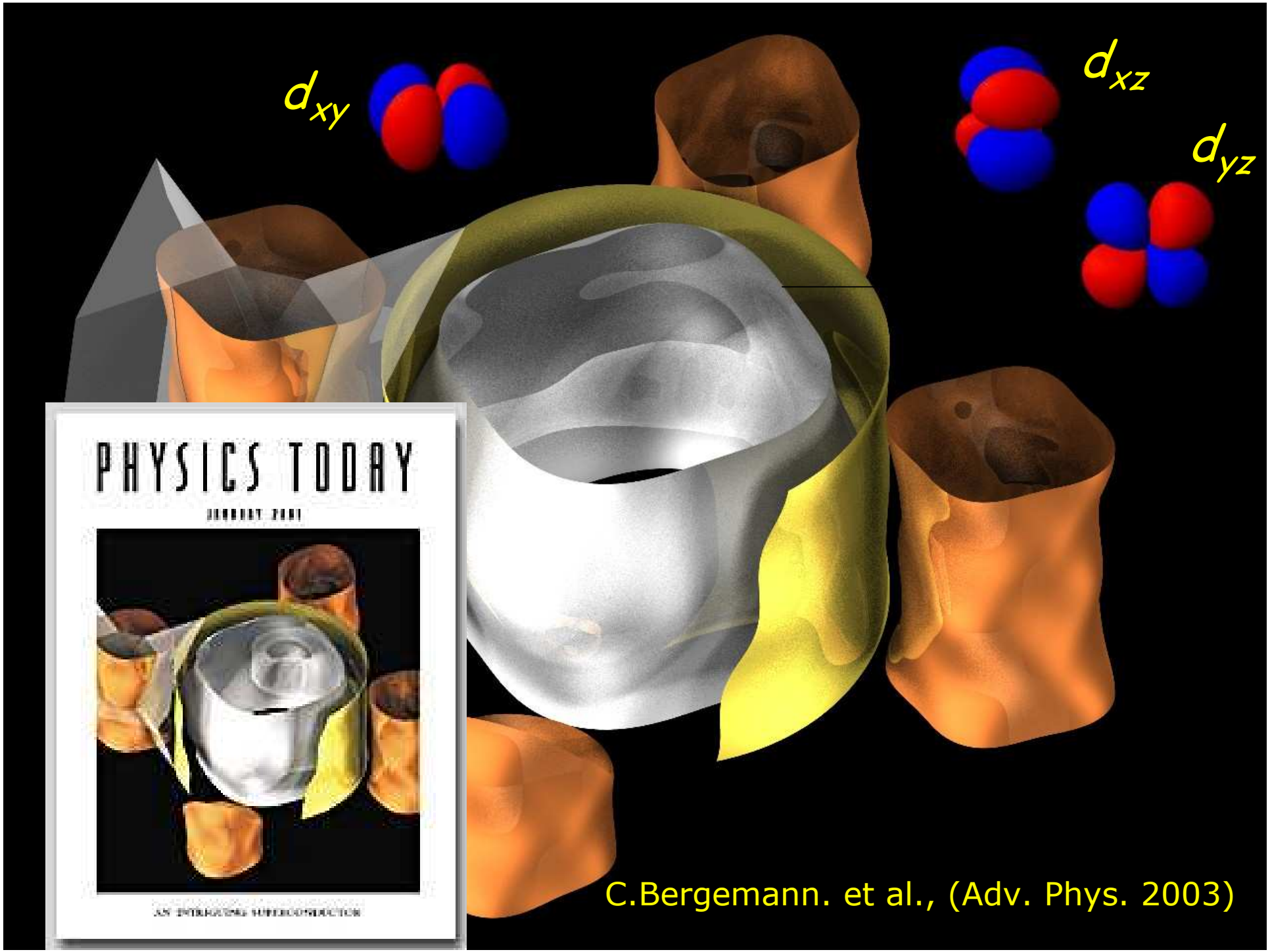
d_{xy}
d_{xz}
d_{yz}
PHYSICS TODAY
C.Bergemann. et al., (Adv. Phys. 2003)

magnetism in Sr_2RuO_4 / inelastic neutron scattering

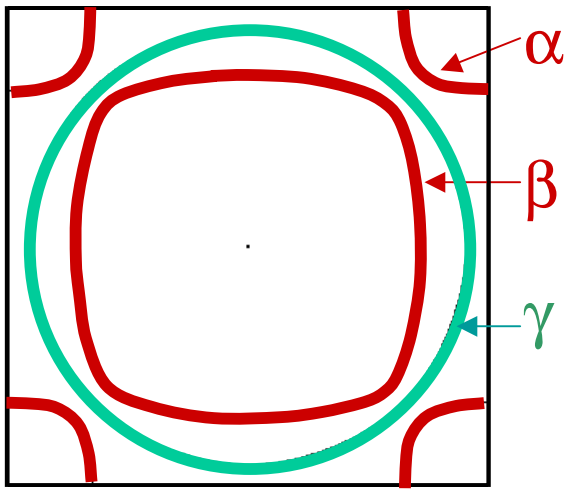

nesting : α/β-Fermi surface

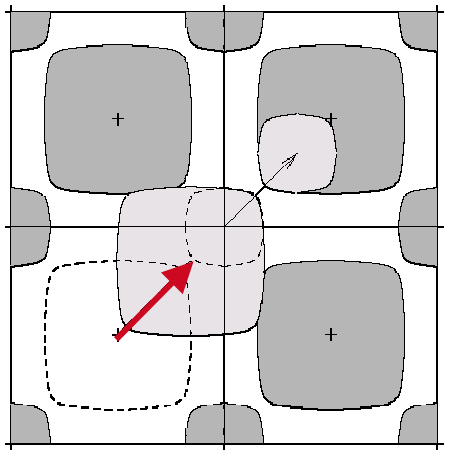

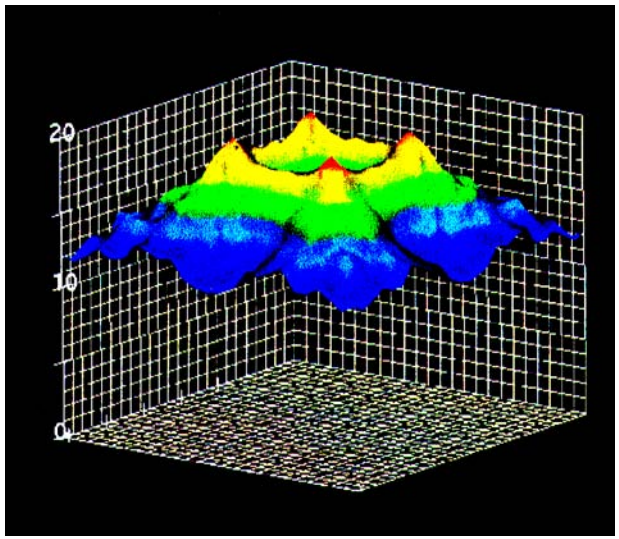

dynamic suszeptibility (RPA)

$$\chi_0(q,\omega) = (g\mu_B)^2 \sum_{k,i,j} \frac{M^{i,j}_{k;(k+q)}[f(\varepsilon_{k,i}) - f(\varepsilon_{(k+q),j})]}{\varepsilon_{(k+q),j} - \varepsilon_{q,i} - \hbar\omega + i0^+}$$

$$\chi(q) = \frac{\chi_0(q)}{1 - I(q)\chi_0(q)}$$

$$I \sim \chi''(\vec{q},\omega)$$

Mazin and Singh , PRL (1999)

Inelastic neutron scattering

neutron sources

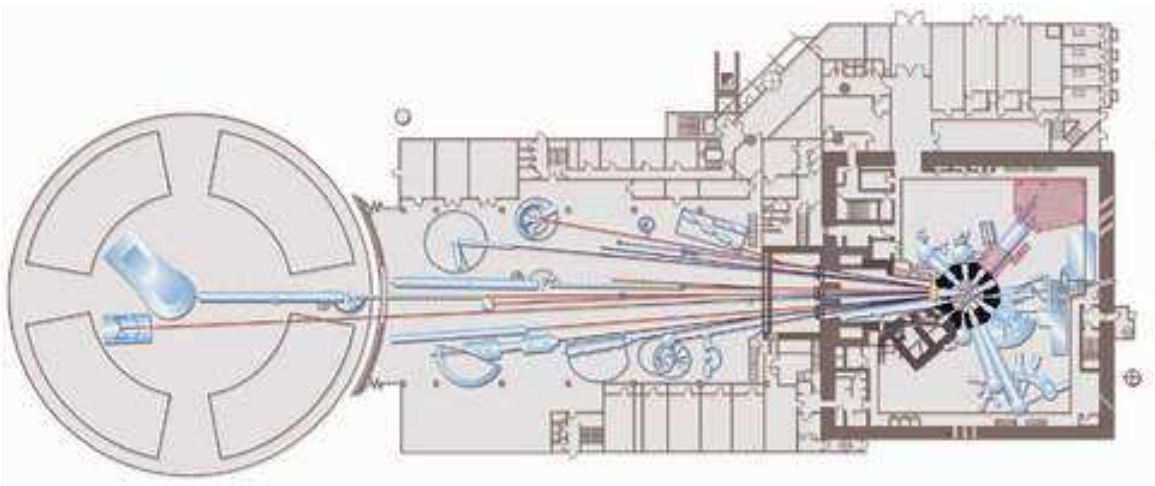

$U^{235}+n \rightarrow Mo^{95}+La^{139}+2n$

235x7.6 95x8.6 138x8.4MeV

i.e. 200 MeV energy

6MeV kinetic energy of the neutron

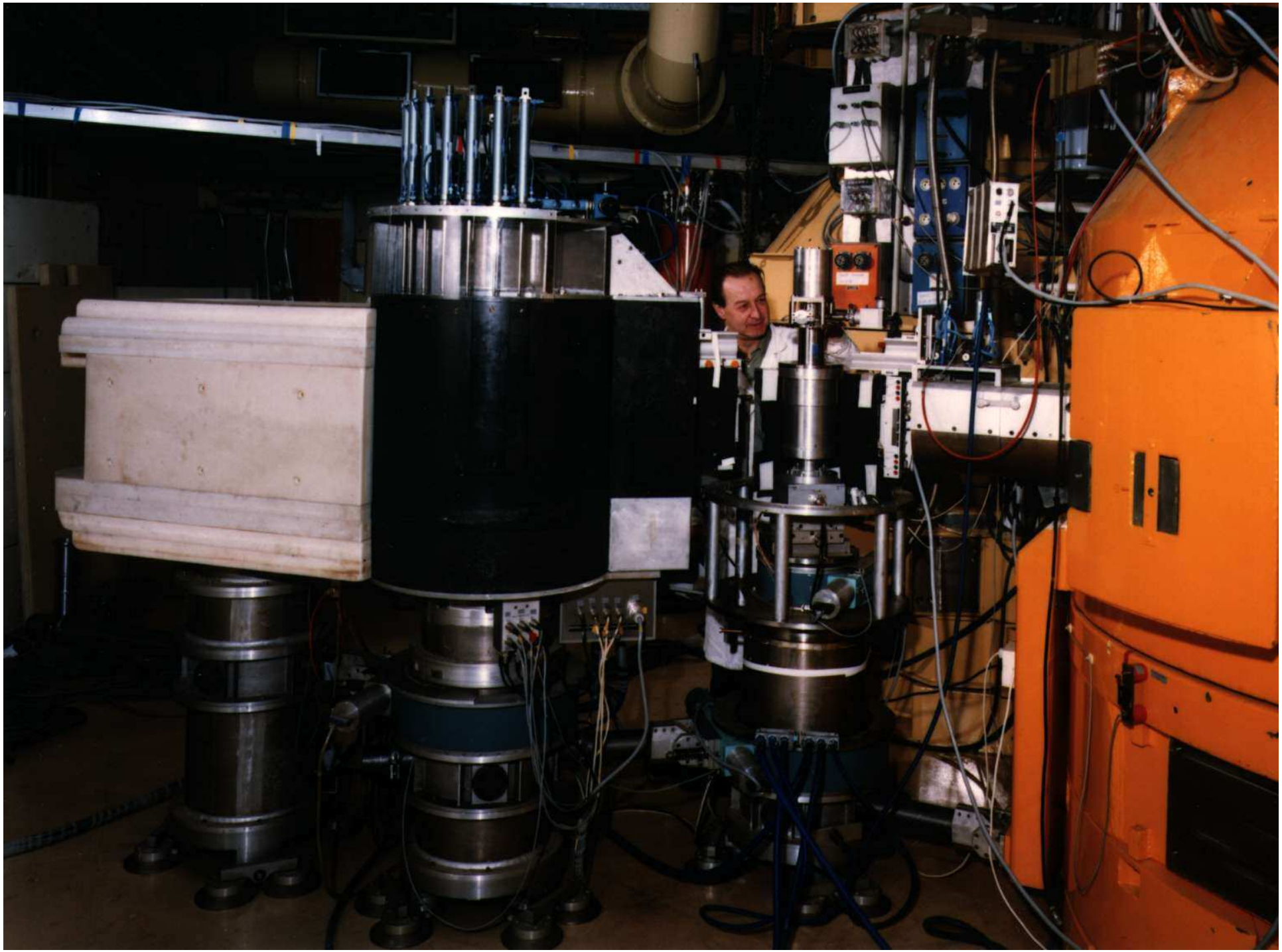

Inelastic neutron scattering

$$\frac{d^2\sigma}{d\Omega d\omega} = r_0^2 \cdot \frac{2F^2(Q)}{\pi(g\mu_B)^2} \cdot \frac{\chi''(Q,\omega)}{1-\exp(-\frac{h\omega}{kt})}$$

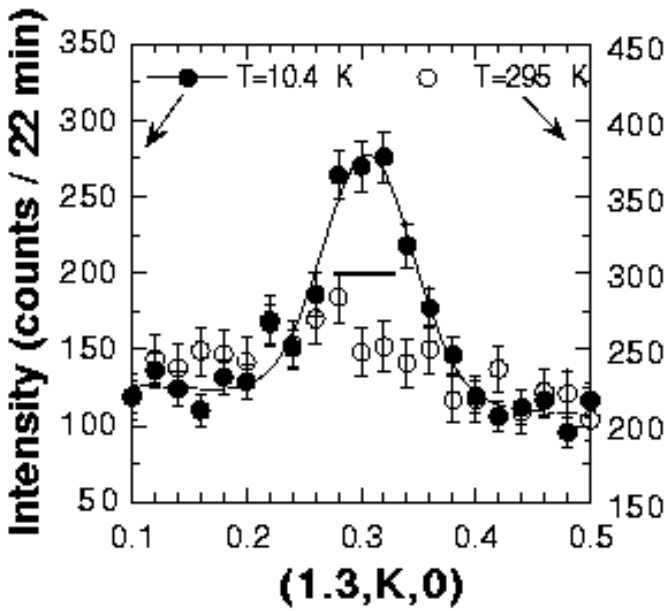

Sidis et al., PRL 1999

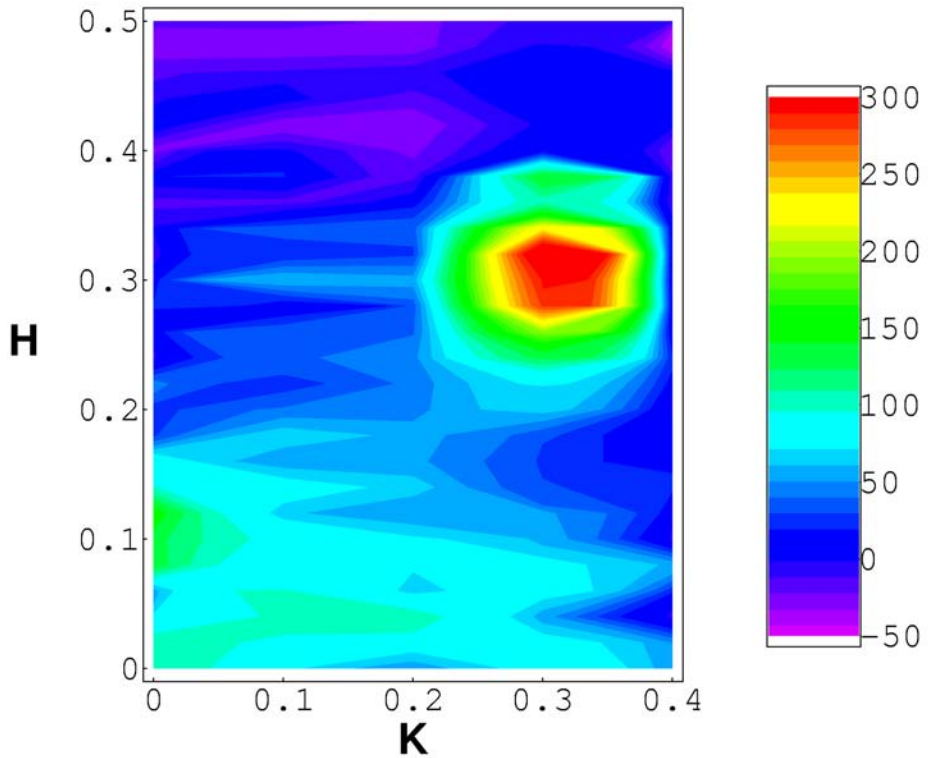

Braden et al., PRB66, 064522 2002; PRL92, 097402, 2004.

- Scans at constant energy, E=6.2meV, along Q=(1.3 y 0) show a clear peak
- incommensurate fluctuations due to nesting in one-dimensional bands

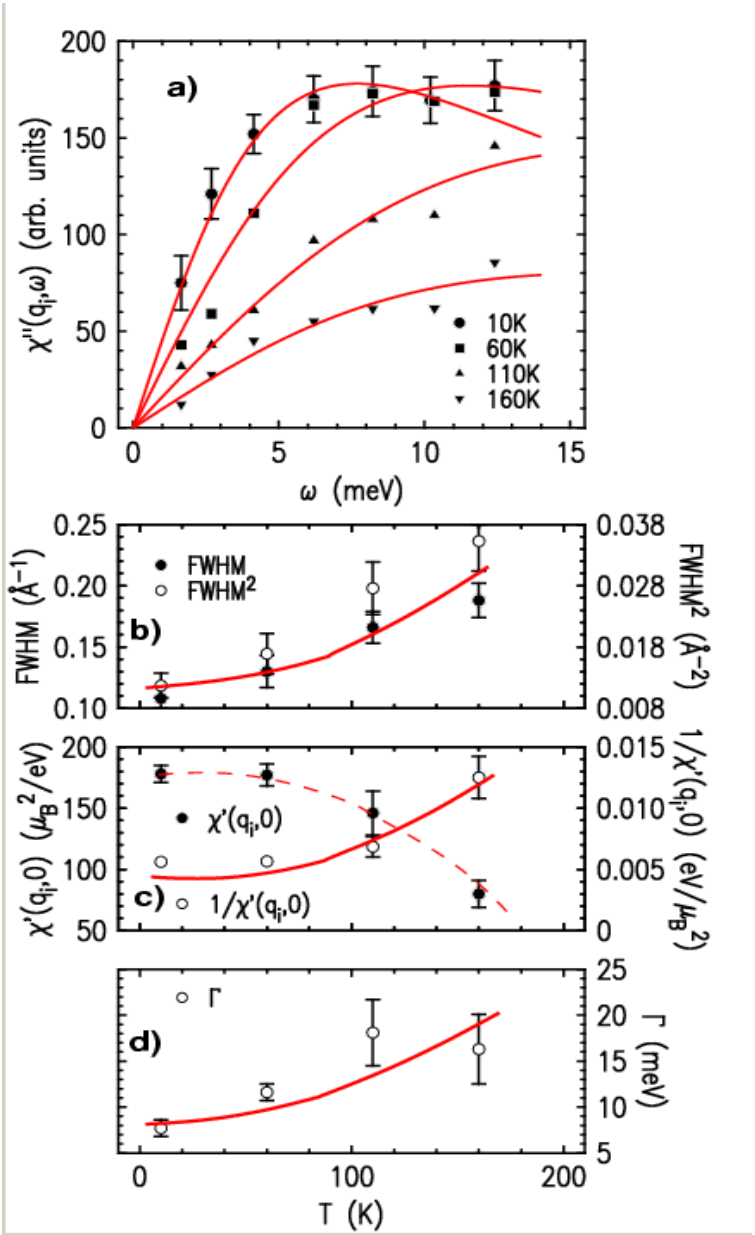

Braden et al., PRB 2002

Energy-Temperature-dependency

$$\chi''(q_i,\omega) = \chi'(q_i,0)\cdot\frac{\Gamma\cdot\omega}{\Gamma^2+\omega^2}$$

- $\chi'(q_0,0)$ and Γ and FWHM vary as function of T
- all indicate a close instability !

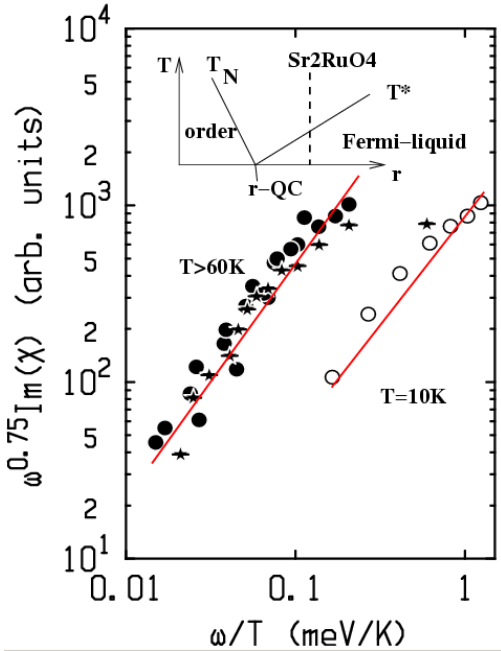

neutron diffraction in Ti-doped Sr_2RuO_4

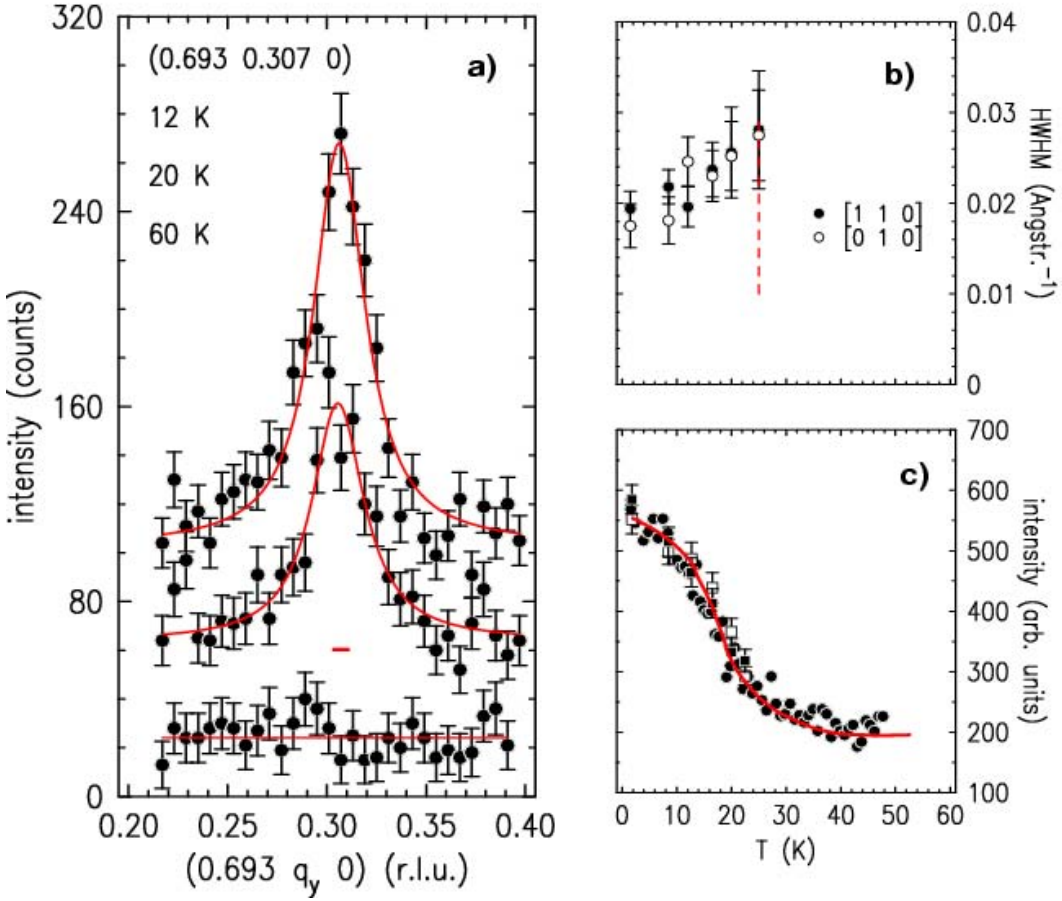

$Sr_2Ru_{1-x}Ti_xO_4$
x=0.09

Braden et al., PRL 88, 2002

- static peaks at the incommensurate positions
- coherence ~40Å

- Sr_2RuO_4 is close to a QCP !

Pairing : Where is the problem ?

- assume : coupling via magnetic excitations
  and weak coupling
  (Fay & Appel; Monthoux & Lonzarich)

- application to Sr_2RuO_4: Mazin&Singh (1999)
  nesting response Ł d-wave SC
  ferromagnetic response Ł p-wave SC
  (Rice &Sigrist)

$$\chi(q) = \frac{\chi_0(q)}{1 - I(q)\chi_0(q)}$$

$$\Updownarrow$$

$$V(q = k - k') = \frac{I^2(q)\chi_0(q)}{1 - I^2(q)\chi_0^2(q)}$$

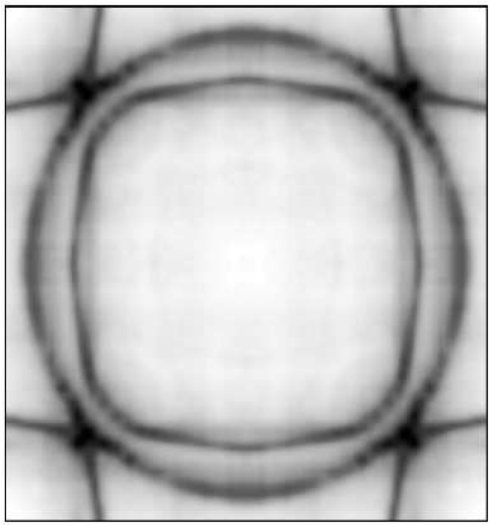

HOWEVER

$d_{x^2-y^2}$ -wave SC inconsistent with experiment
also d_{xy}-band should be active !!!

full spectrum Ł superconducting order parameter

ferromagnetic fluctuations in Sr_2RuO_4 polarized neutron scattering

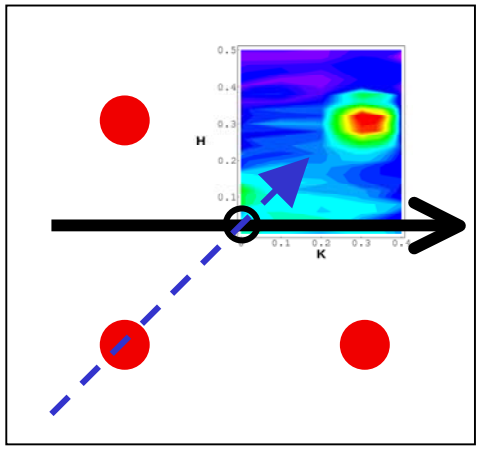

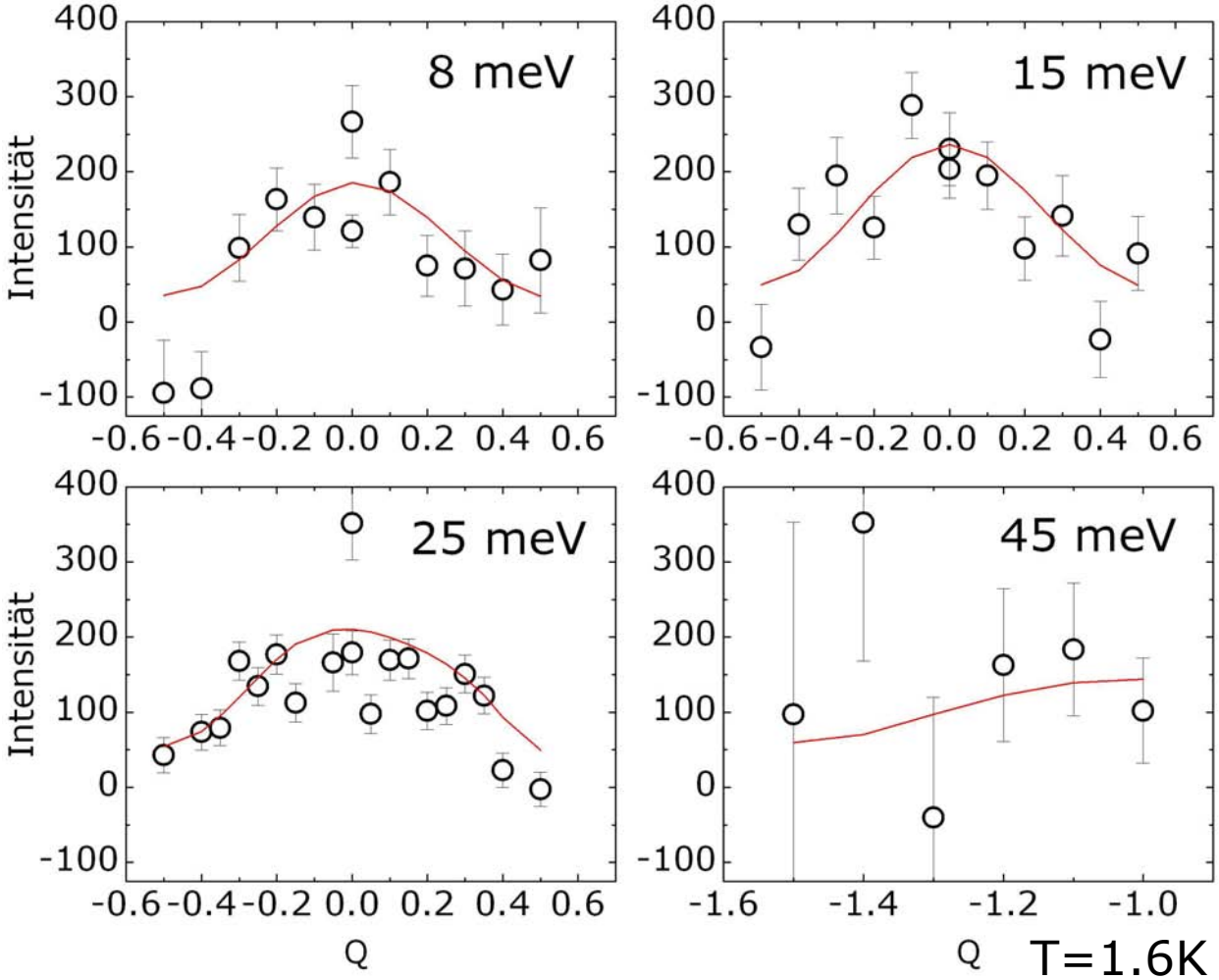

Diagonal

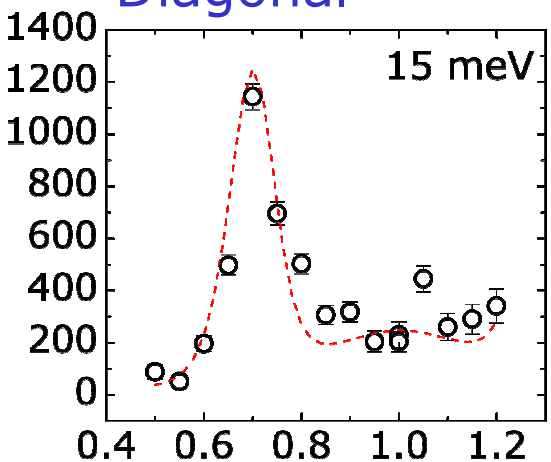

There is a weak FM component

ferromagnetic fluctuations in Sr_2RuO_4

model : $\chi'(q)$

Γ = 15.5 ± 1.4 meV

W = 0.53 ± 0.04 r.l.u.

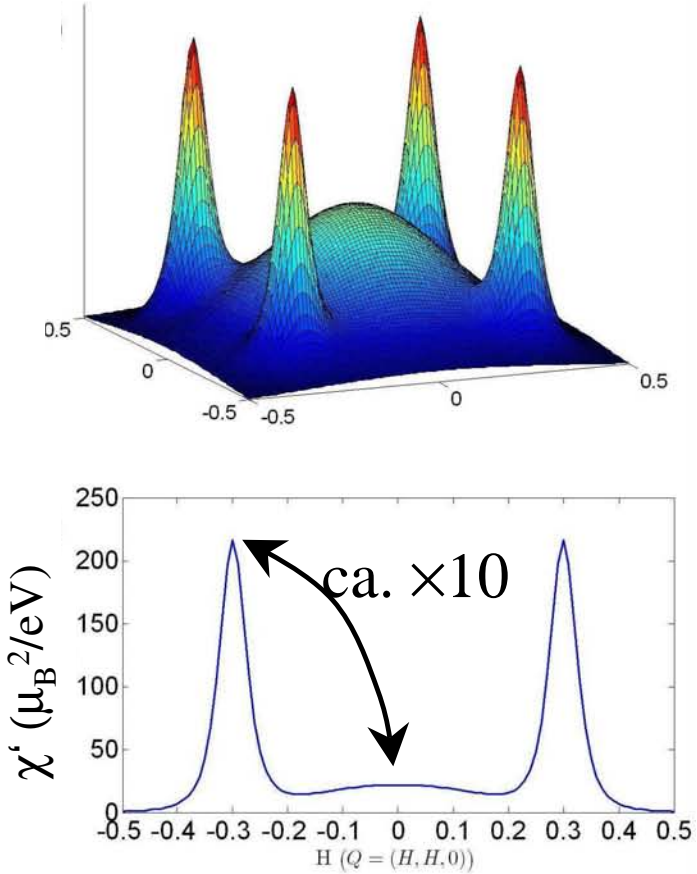

quantitative agreement:

- NMR
- specific heat γ
- suszeptibility (q=0)

Ca_2RuO_4

$Ca_{2-x}Sr_xRuO_4$

Sr_2RuO_4

Ca

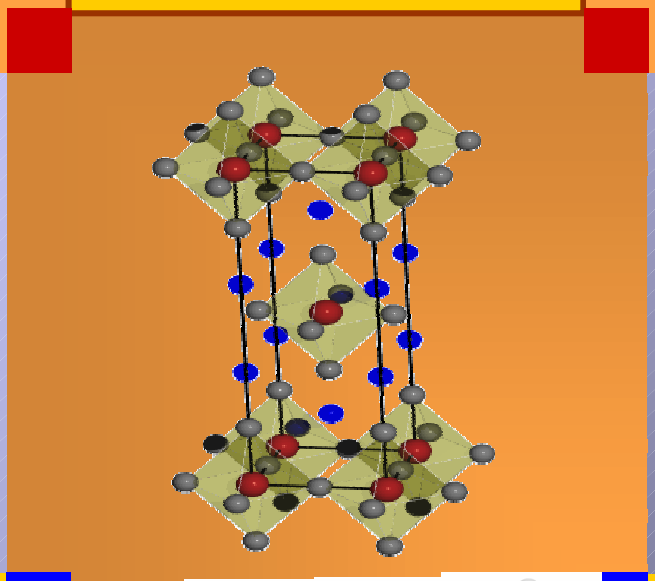

Sr

Ca_3Ru_2O

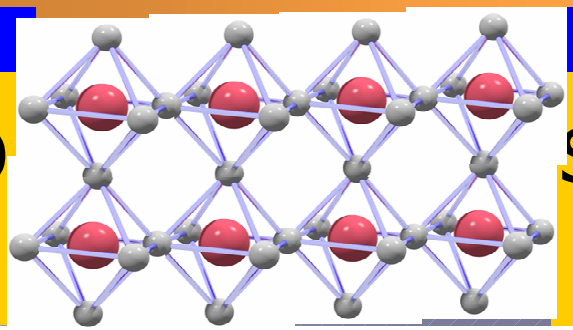

$Sr_3Ru_2O_7$

$Ca_{2-x}Sr_xRuO_4$ Structural properties

Isovalent substitution

$r_{Ca} < r_{Sr}$

Ca^{2+}
r = 1.18Å

↔

Sr^{2+}
r = 1.31Å

complex phase diagram

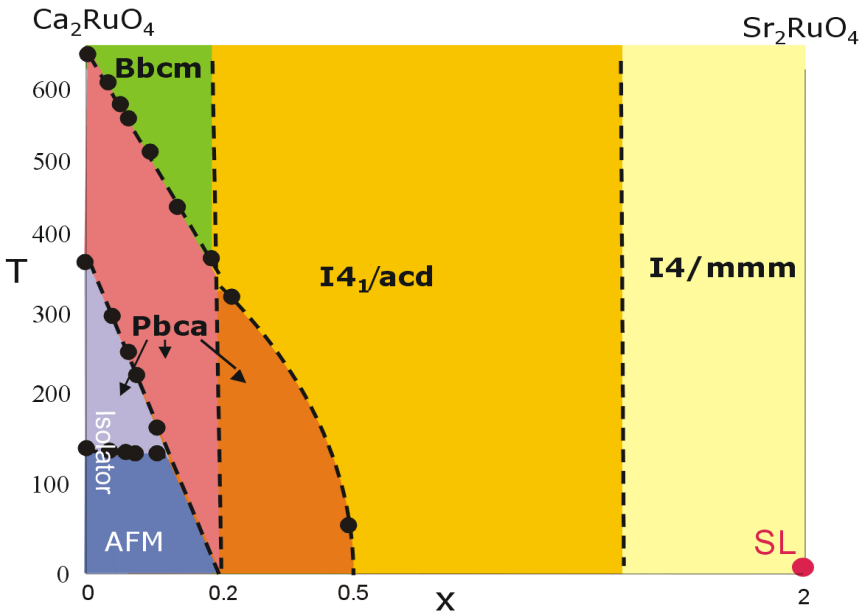

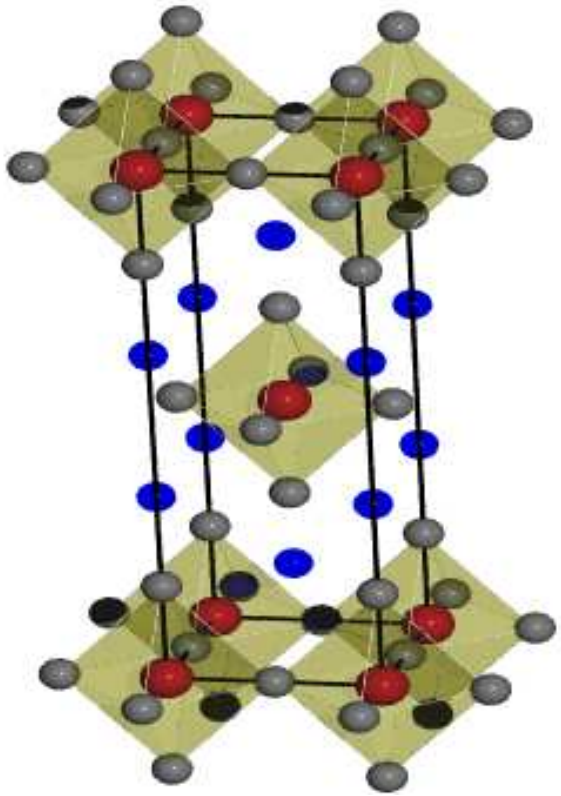

Nakatsuji et al. PRL 84 2666 (2000), Friedt et al. PRB 63, 174432 (2001), Braden et al. PRB 58, 847 (1998)

Structural distortions in $Ca_{2-x}Sr_xRuO_4$

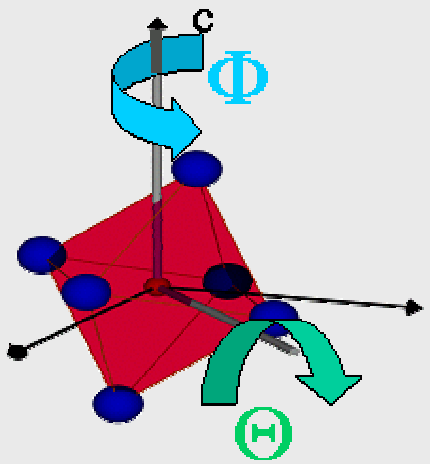

tilt
|| edges

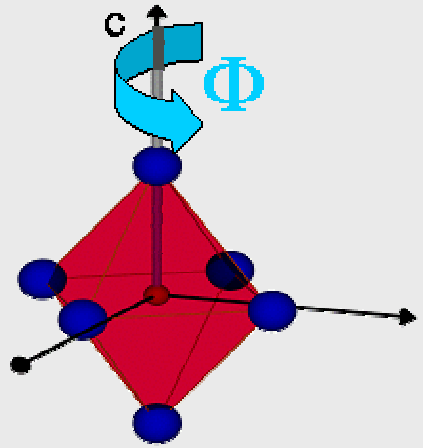

rotation
around c-axis

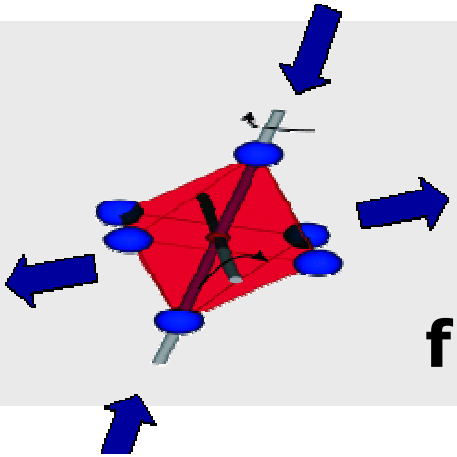

flattening

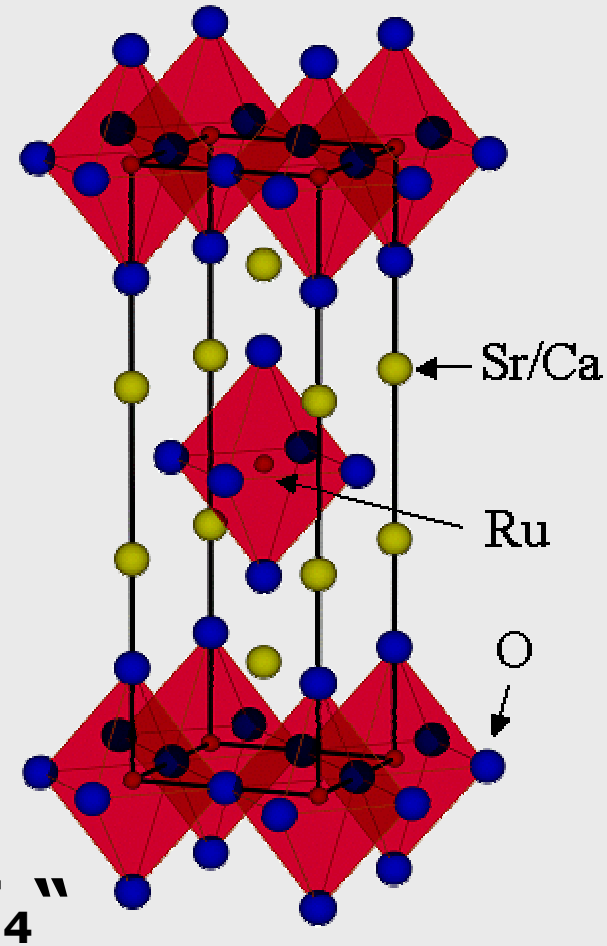

„K_2NiF_4"
(undistorted)

Tilt distortion

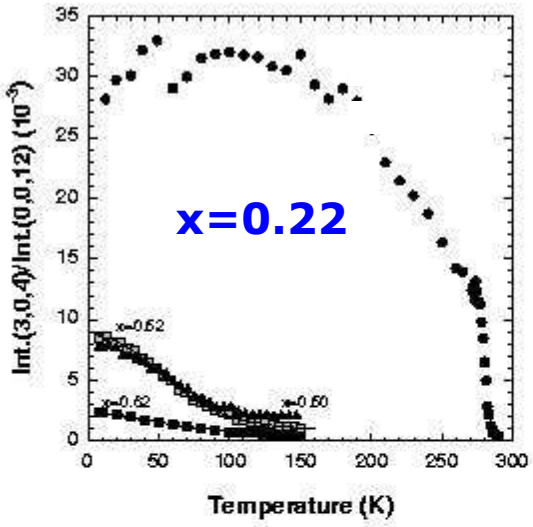

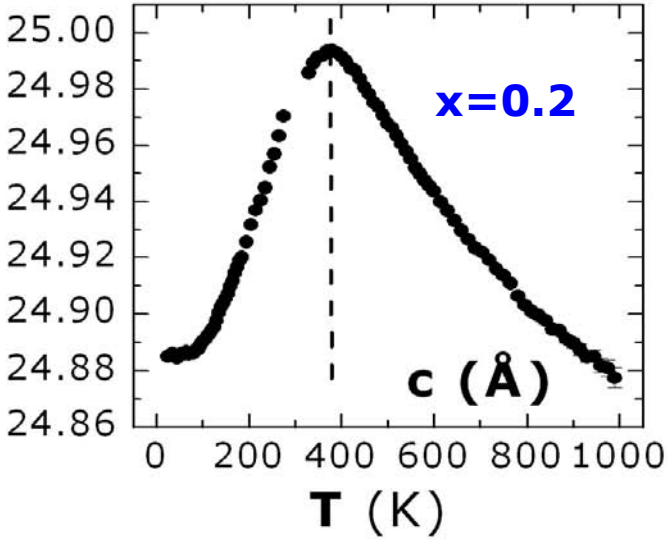

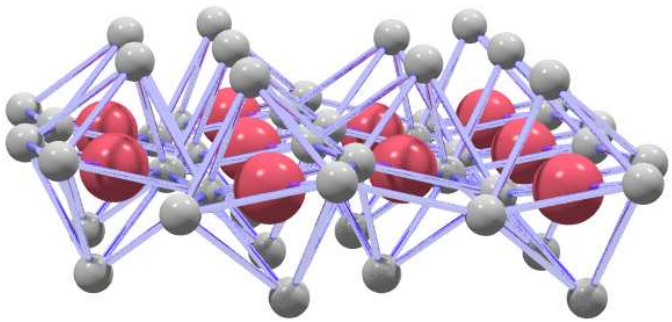

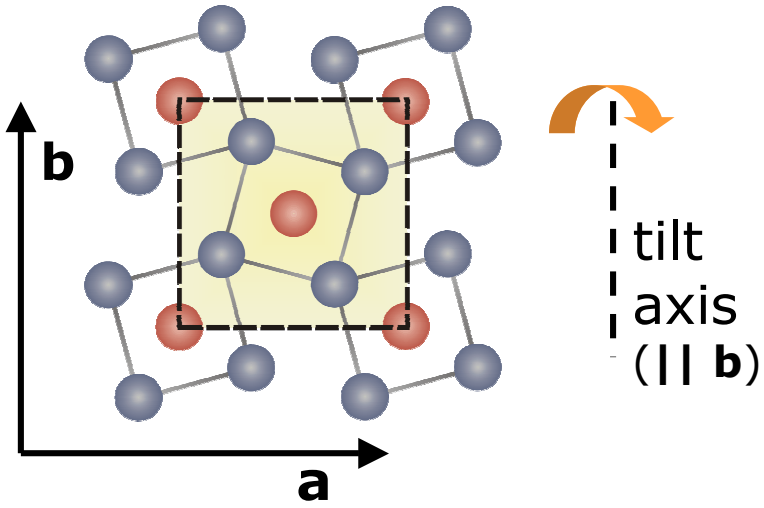

- **tilt stacking sequence always one c !**

Space group **Pbca**

Stacking sequence : rotation

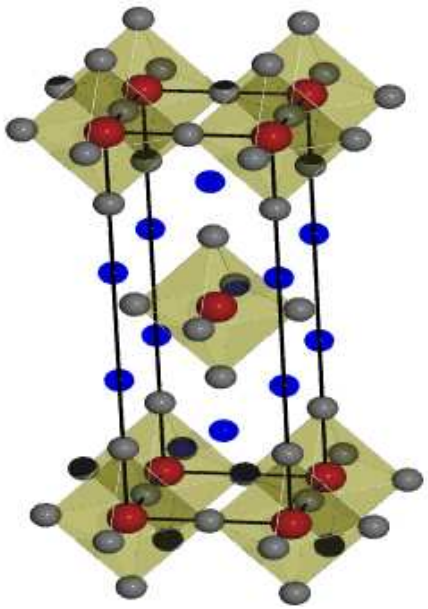

2 / 4 – fold
Symmetry at Ru-site

Different ground
State (orbital order)

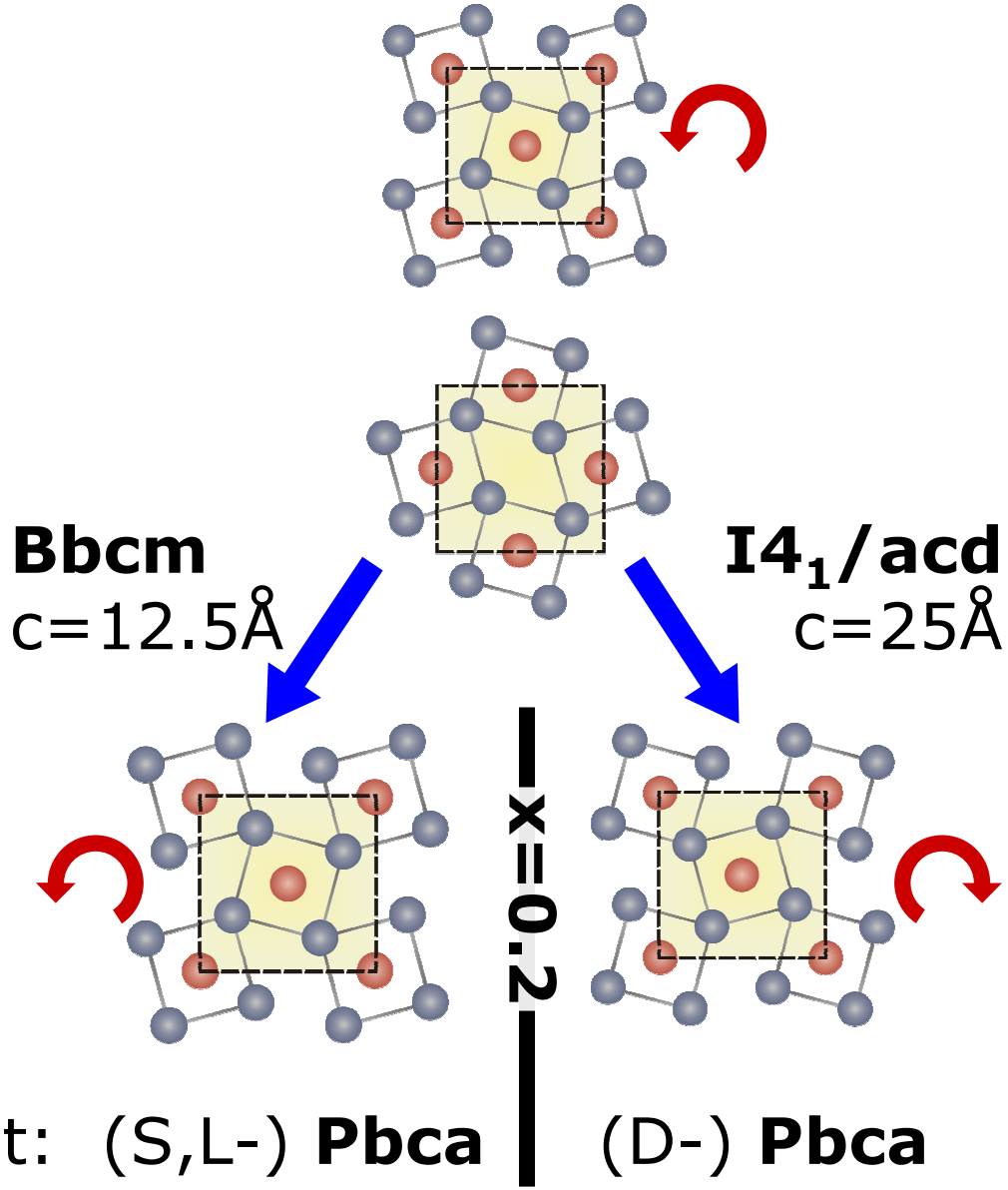

$Ca_{2-x}Sr_xRuO_4$ Structural properties

Isovalent substitution

$r_{Ca} < r_{Sr}$

Ca^{2+}
r = 1.18Å

↔

Sr^{2+}
r = 1.31Å

complex phase diagram

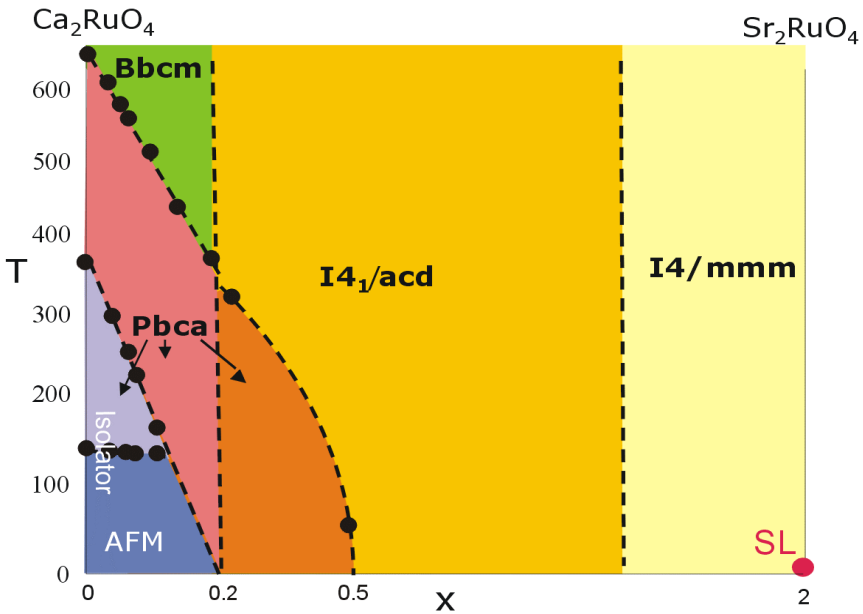

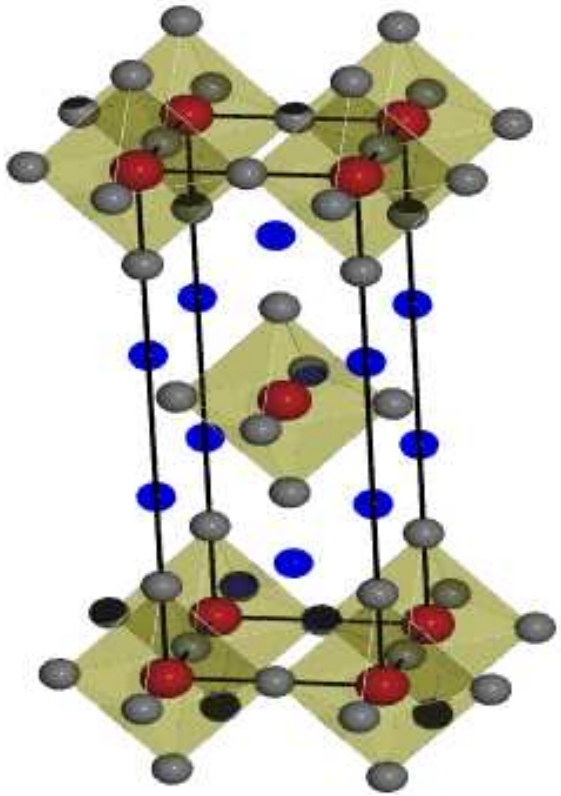

Nakatsuji et al. PRL 84 2666 (2000), Friedt et al. PRB 63, 174432 (2001), Braden et al. PRB 58, 847 (1998)

Metal-insulator-transition in Ca_2RuO_4

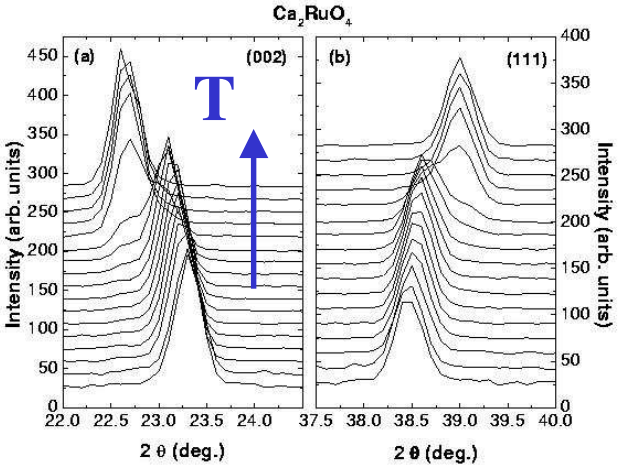

Friedt et al. PRB 63, 174432 (2001),
Braden et al. PRB 58, 847 (1998)

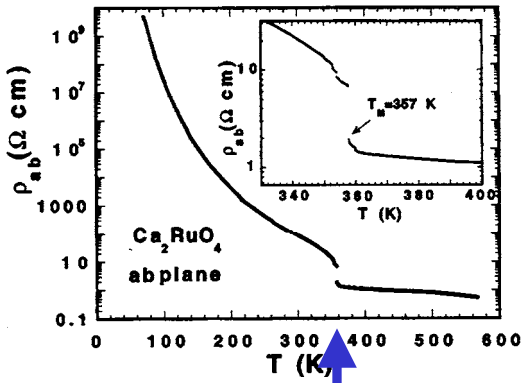

Alexander et al., PRB 2000

Nakatsuji et al., PRB 2001
PRL 2000

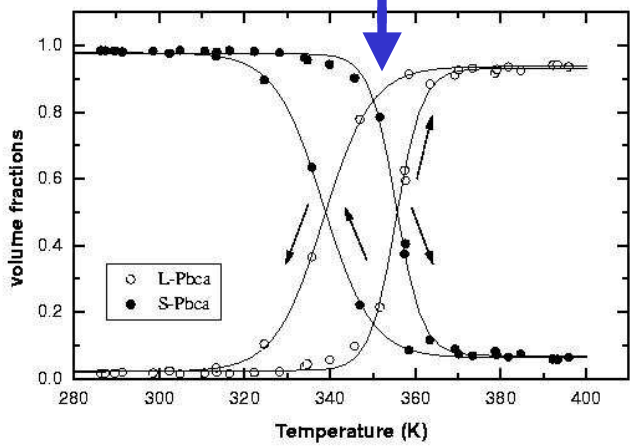

symmetry in metallic AND in insulating phases
Pbca : one-c tilt plus one-c rotation

Antiferromagnetic order in Ca_2RuO_4

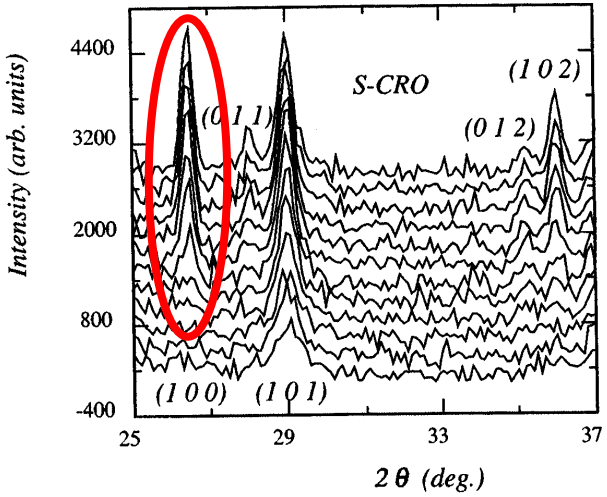

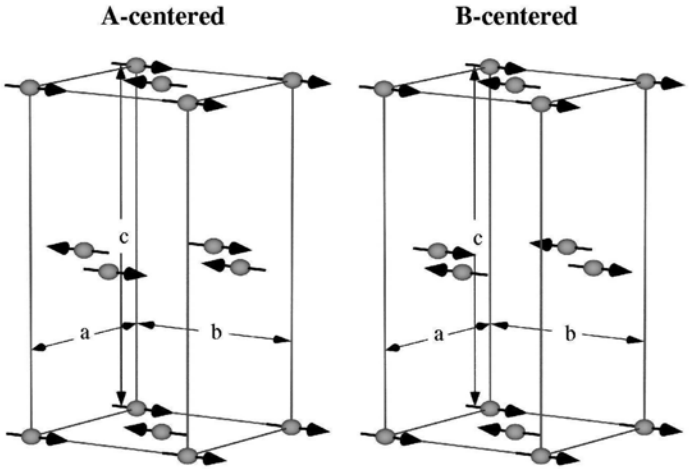

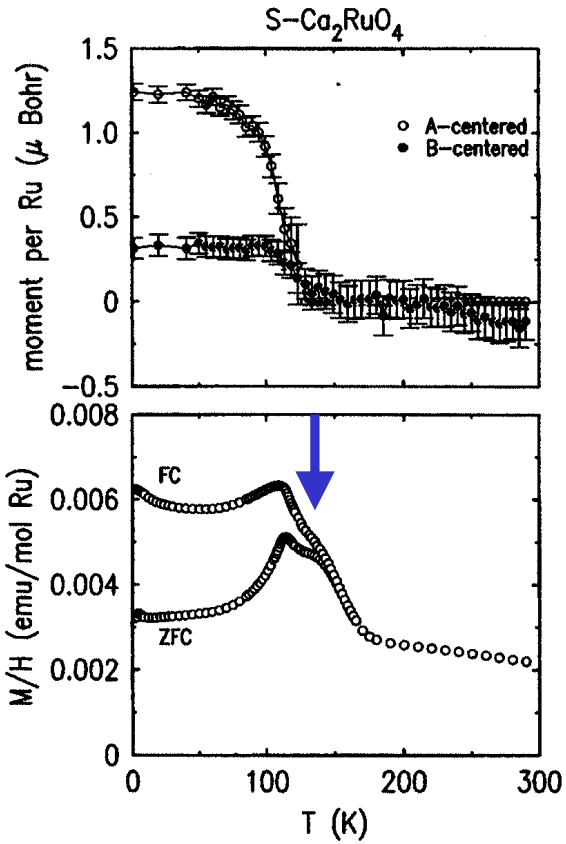

- **two magnetic ordering schemes in a nearly stoichiometric powder**
- **best crystals only A-centering T_N~110K**
- **excess oxygen or Sr-substitution : B-centering T_N~150K**

MI-transition : orbital effects

- **orbital occupation changes : at MI-transition & in insulating phase**

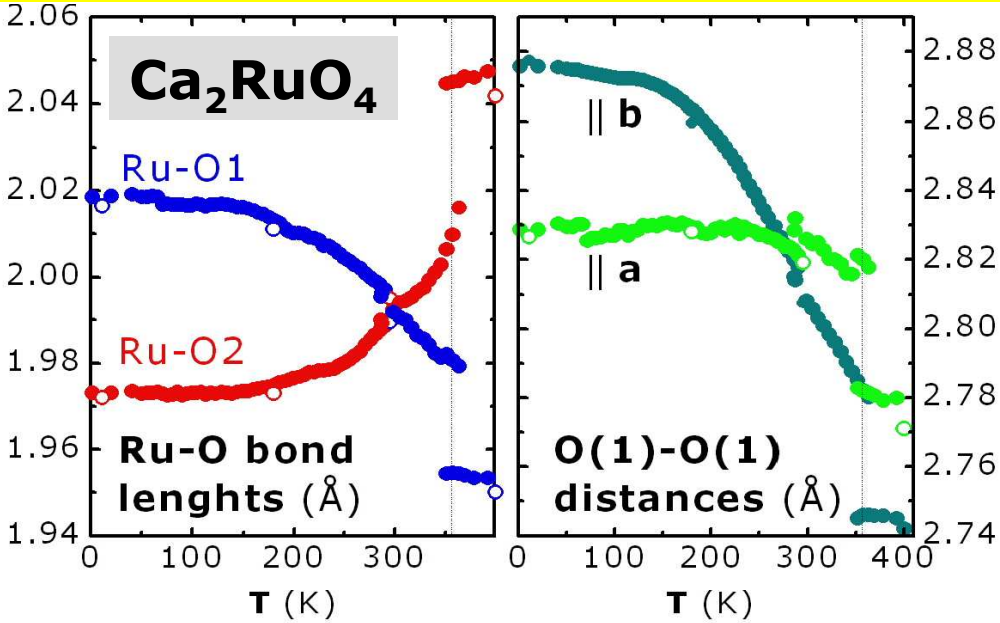

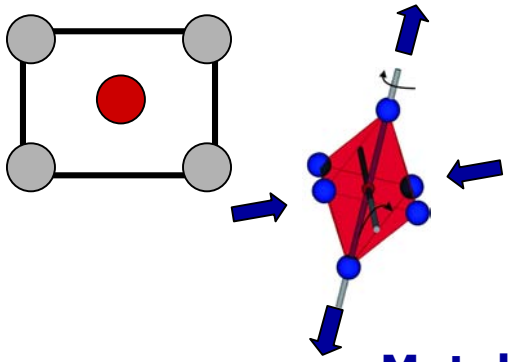

Metallic:
Elongated octahedron

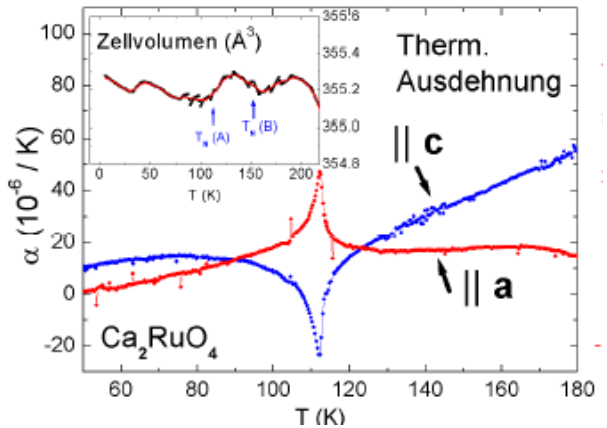

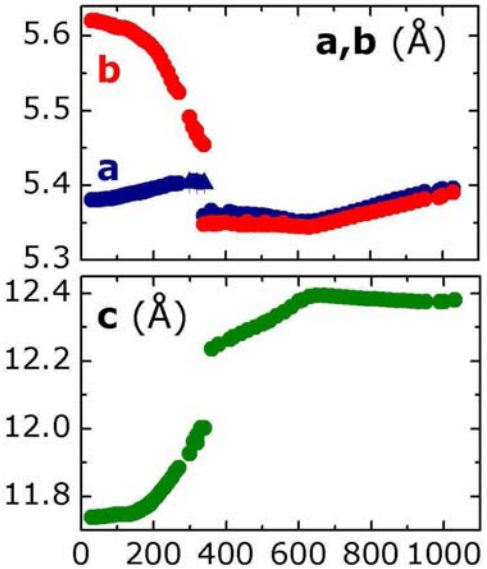

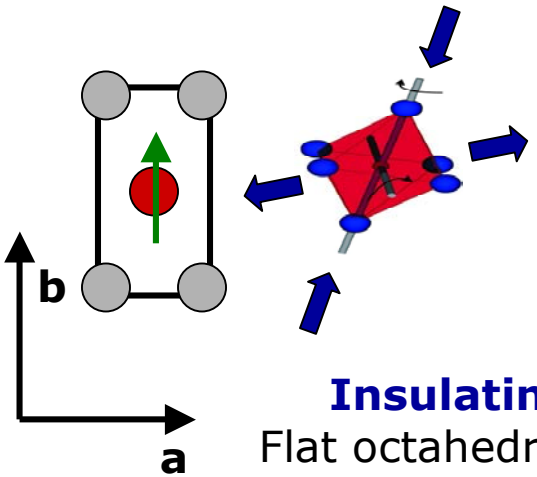

Insulating:
Flat octahedron
e^- d_{xy}-band

Friedt et al. PRB 63, 174432 (2001),
Braden et al. PRB 58, 847 (1998)
Steffens et al. PRB 72,094104 (2005).

Orbital effects in Ca_2RuO_4

1. **Orbital-Selective Mass Enhancements in Multiband *Ca*2-*x*Sr*x*Ru*O*4 Systems Analyzed by the Extended Drude Model** J. S. Lee et al. , Phys. Rev. Lett. **96**, 057401 (2006)
2. **Strong Orbital-Dependent *d*-Band Hybridization and Fermi-Surface Reconstruction in Metallic *Ca*2-*x*Sr*x*Ru*O4** Eunjung Ko et al., Phys. Rev. Lett. **98**, 226401 (2007)
3. **Subband Filling and Mott Transition in *Ca*2-*x*Sr*x*Ru*O*4** A. Liebsch et al. Phys. Rev. Lett. **98**, 216403 (2007)
4. **Orbital Ordering Transition in *Ca*2*Ru*O*4 Observed with Resonant X-Ray Diffraction** I. Zegkinoglou et al., PR.L. **95**,136401 (2005)
5. **Ferro-Type Orbital State in the Mott Transition System *Ca*2-*x*Sr*x*Ru*O*4 Studied by the Resonant X-Ray Scattering Interference Technique** M. Kubota et al., Phys. Rev. Lett. **95**, 026401 (**2005)**
6. **Lattice dynamics and the electron-phonon interaction in *Ca*2*Ru*O*4** H. Rho et al., Phys. Rev. B **71**, 245121 (2005)
7. **Orbital-Selective Mott Transitions in the Degenerate Hubbard Model** Akihisa Koga et al., Phys. Rev. Lett. **92**, 216402 (2004)
8. **Correlation effects in *Sr*2*Ru*O*4 and *Ca*2*Ru*O*4 : Valence-band photoemission spectra and self-energy calculations** T. T. Tran et al., Phys. Rev. B **70**, 153106 (2004)
9. **Orbital-dependent phase control in Ca2-*x*Sr*x*RuO4 (0<~*x*<~0.5**) Zhong Fang et al., Phys. Rev. B **69**, 045116 (2004)
10. **Orbital state and metal-insulator transition in Ca2-*x*Sr*x*RuO4 (*x*=0.0 and 0.09) studied by x-ray absorption spectroscopy** T. Mizokawa et al. , Phys. Rev. B **69**, 132410 (2004)
11. **Raman scattering studies of spin, charge, and lattice dynamics in Ca2-*x*Sr*x*RuO4 (0<~*x*<0.2)** H. Rho et al., PRB **68**, 100404 (2003)
12. **Change of Electronic Structure in Ca2RuO4 Induced by Orbital Ordering** J. H. Jung et al., Phys. Rev. Lett. **91**, 056403 (2003)
13. **Electron and Orbital Correlations in Ca2-*x*Sr*x*RuO4 Probed by Optical Spectroscopy** J. S. Lee et al, PRL. **89**, 257402 (2002)
14. **Orbital state and metal-insulator transition in Ca2-*x*Sr*x*RuO4 studied by model Hartree-Fock calculations** M. Kurokawa et al. Phys. Rev. B **66**, 024434 (2002)
15. **Pressure-Tuned Collapse of the Mott-Like State in Ca*n*+1Ru*n*O3*n*+1 (*n*=1,2): Raman Spectroscopic Studies** C. S. Snow et al., Phys. Rev. Lett. **89**, 226401 (2002)
16. **Prediction of Orbital Ordering in Single-Layered Ruthenates** Takashi Hotta and Elbio Dagotto Phys. Rev. Lett. **88**, 017201 (2002)
17. **From Mott insulator to ferromagnetic metal: A pressure study of Ca2RuO4** Fumihiko Nakamura et al., PRB **65**, 220402 (2002)
18. **Spin-Orbit Coupling in the Mott Insulator *Ca*2*Ru*O*4** T. Mizokawa et al. Phys. Rev. Lett. **87**, 077202 (2001)
19. **Magnetic phase diagram of Ca2-*x*Sr*x*RuO4 governed by structural distortions** Z. Fang Phys. Rev. B **64**, 020509 (2001)
20. **Quasi-Two-Dimensional Mott Transition System *Ca*2-*x*Sr*x*Ru*O*4** S. Nakatsuji et al. Phys. Rev. Lett. **84**, 2666 (2000)
21. **Electronic structure of Ca2RuO4: A comparison with the electronic structures of other ruthenates** L. M. Woods PRB **62**, 7833 (2000)
22. **Ground-state instability of the Mott insulator Ca2RuO4: Impact of slight La doping on the metal-insulator transition and magnetic ordering** G. Cao et al., Phys. Rev. B **61**, R5053 (2000)
23. **Destruction of the Mott insulating ground state of Ca2RuO4 by a structural transition** C. S. Alexander et al., PRB **60**, R8422 (1999)
24. **Layered Ruthenium Oxides: From Band Metal to Mott Insulator** A. V. Puchkov et al., Phys. Rev. Lett. **81**, 2747 (1998)

metal-insulator-transition as function of doping

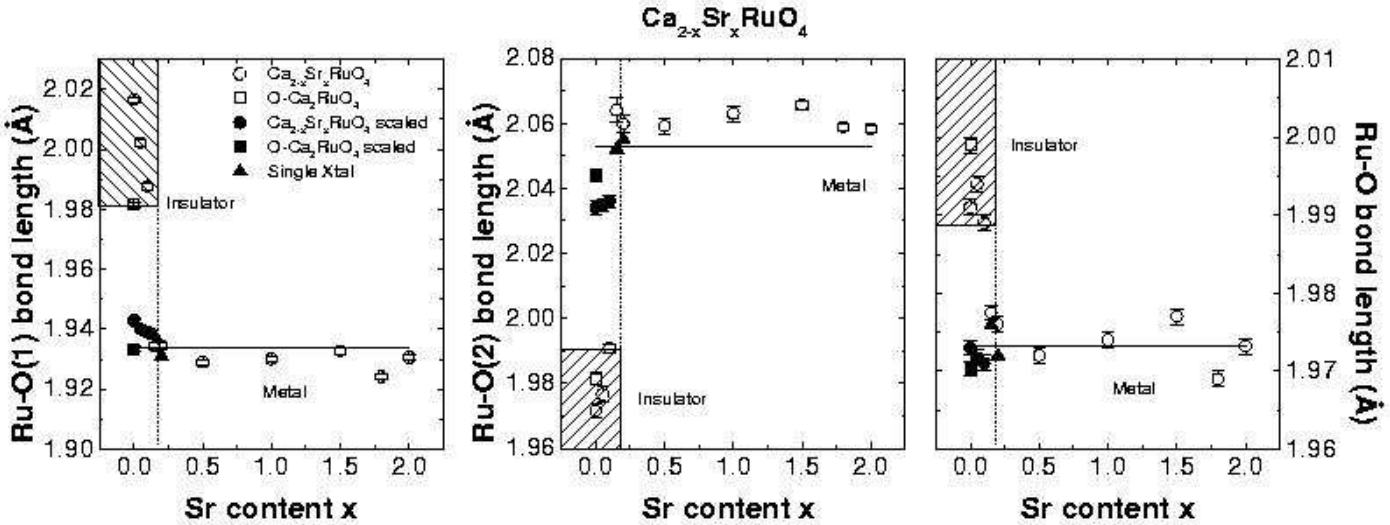

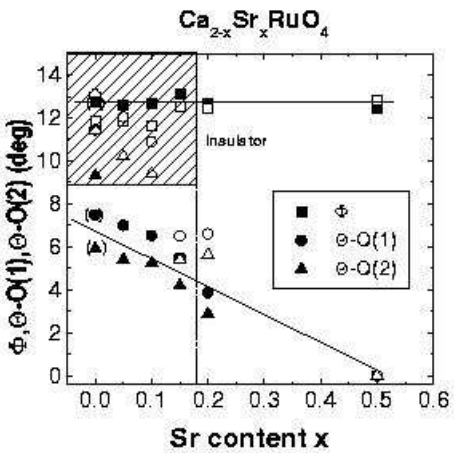

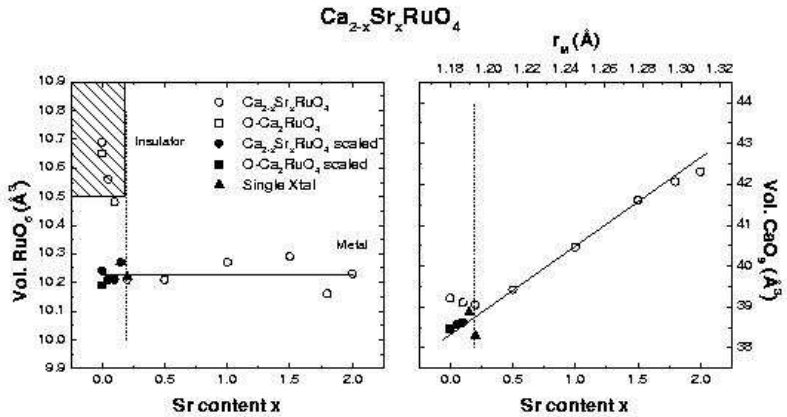

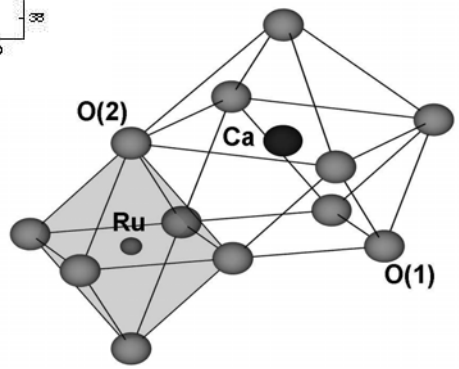

metallic compounds are all very similar :
small tilt & elongated & small RuO-volume

anomalous metals close to MI transition

Braden et al., PRB 1998, Friedt et al., PRB 2001, Nakatsuji PRB 2000, PRL 200, JPSJ 1997.

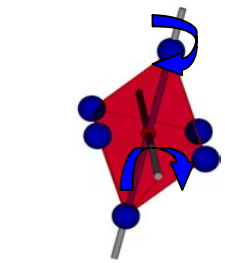

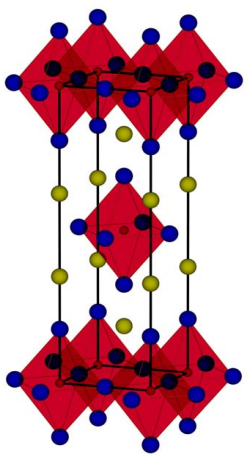

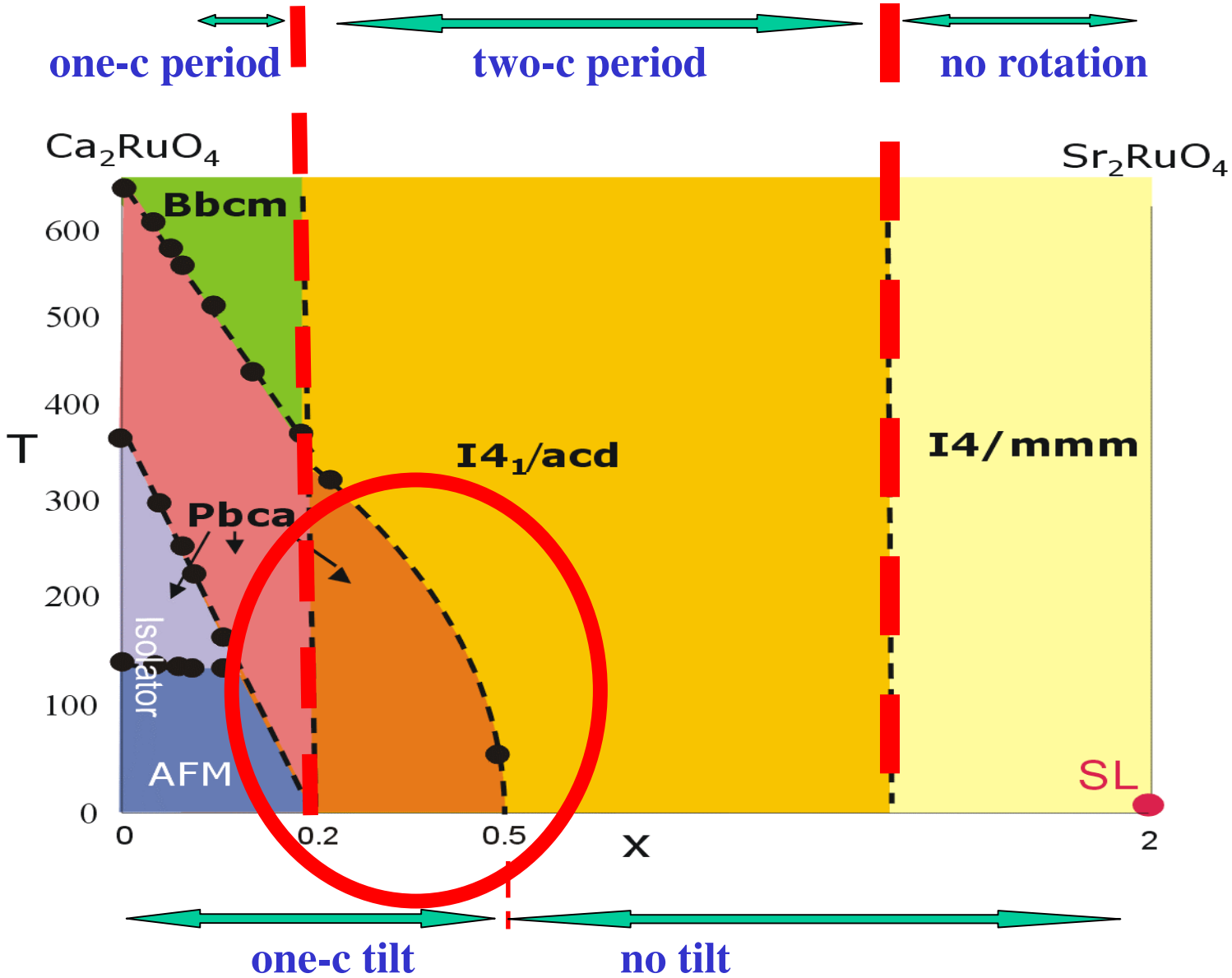

magneto-elastic coupling : 0.2<x<1.5

critical point

of the structural transition

S. Nakatsuji and Y. Maeno
PRB, PRL (2000)

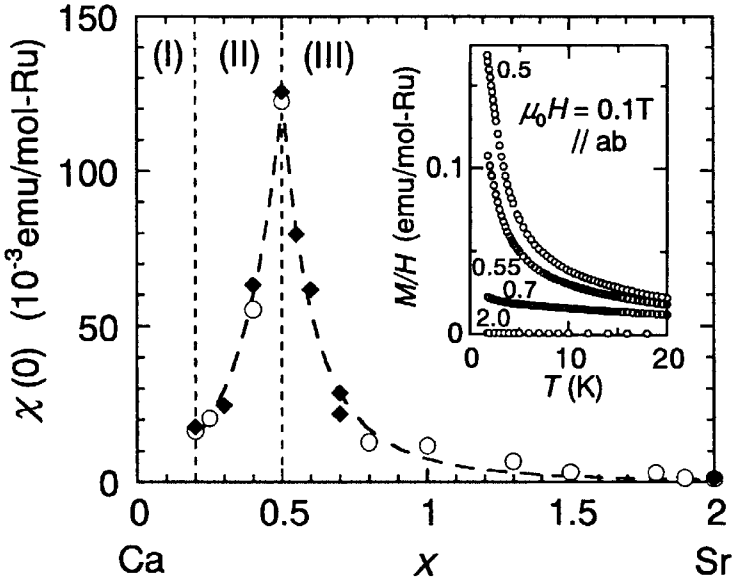

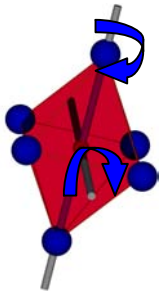

Tilt distortion

Rotational distortion

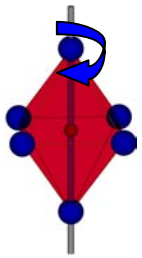

O. Friedt et al., PRB 63, 174432 (2001)

$Ca_{1.5}Sr_{0.5}RuO_4$ x=0.5

- large susceptibility
  $200 \cdot \chi(Sr_2RuO_4)$
- large C_p/T-ratio
  250 mJ/mol $\cdot K^2$

Magneto-elastic coupling : x ~ 0.2

critical point

of the structural transition

S. Nakatsuji and Y. Maeno
PRB, PRL (2000)

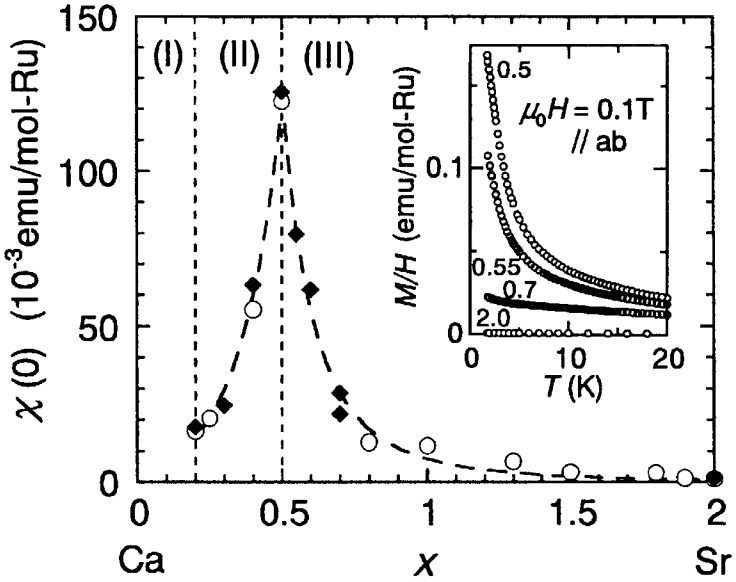

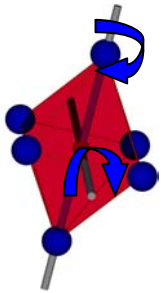

Tilt distortion

Rotational distortion

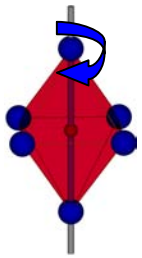

O. Friedt et al., PRB 63, 174432 (2001)

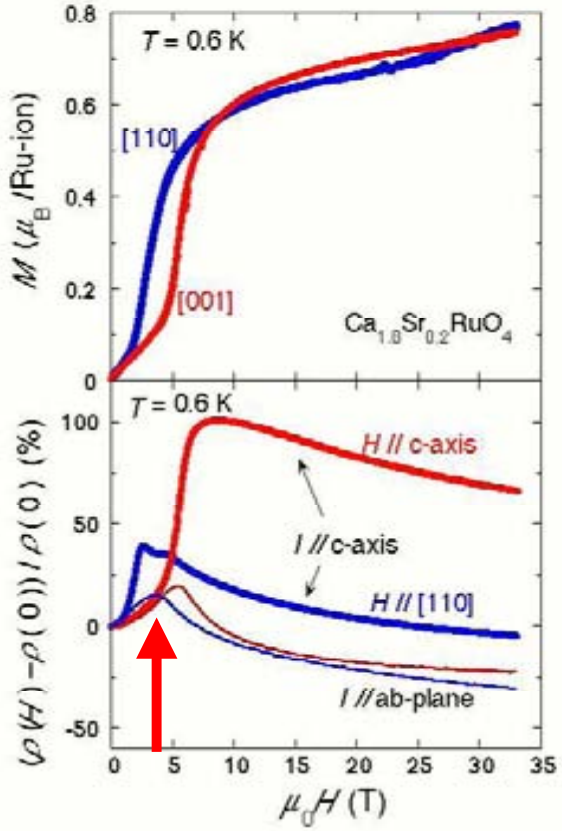

S. Nakatsuji, *et al.*, PRL 2003.

metamagnetism !

Magnetization density

Polarized neutrons (5C1)
Maximum Entropy method (MEM)

x=0.2

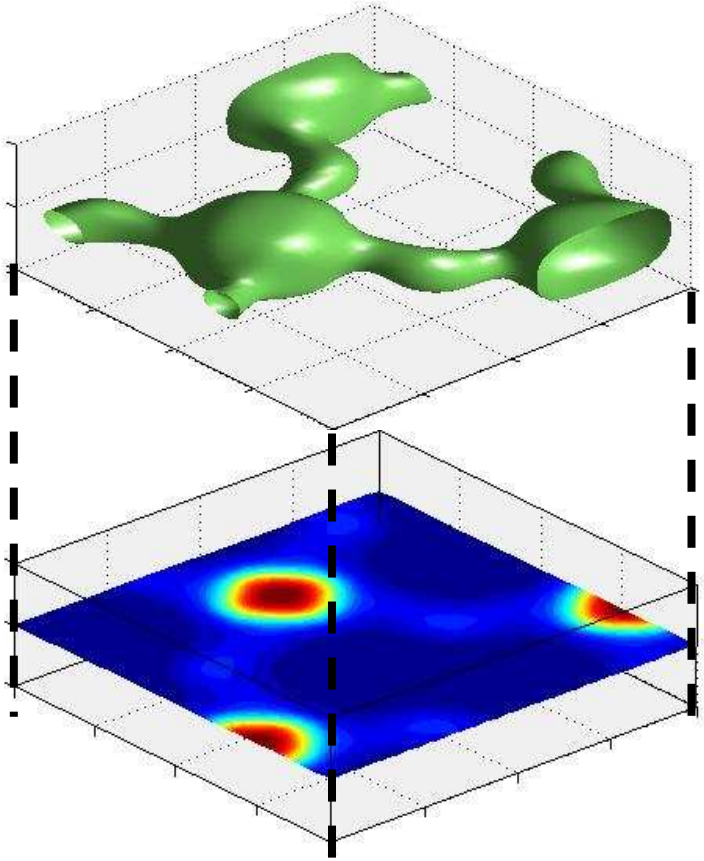

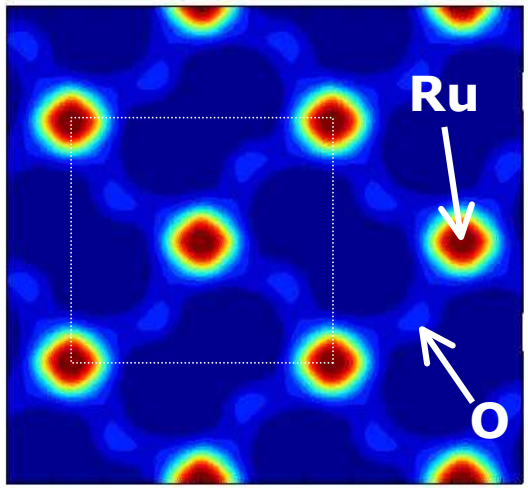

x=0.5

d_{xy}

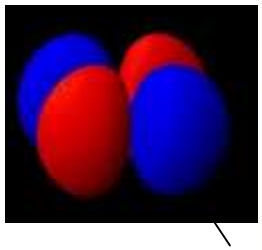

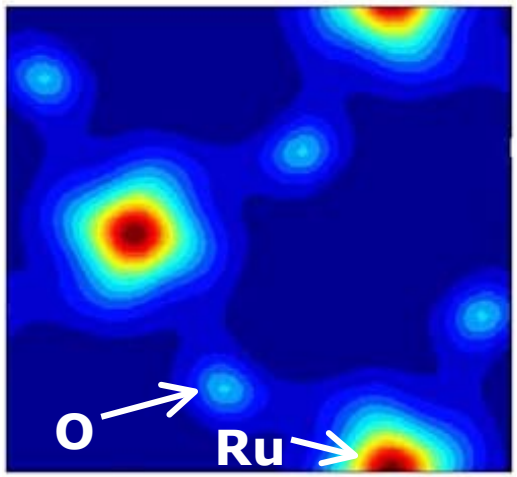

Spin-density: d_{xy}-character

Gukasov et al. PRL 89 (2002)

structural anomalies in $Ca_{1.8}Sr_{0.2}RuO_4$

- **temperature dependencies indicate crossover**

Susceptibility

resistivity

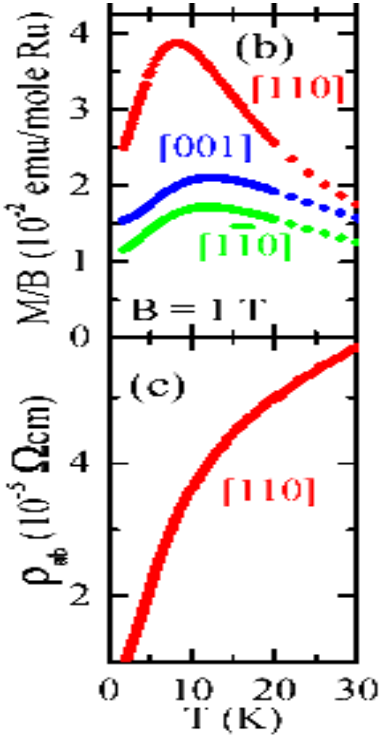

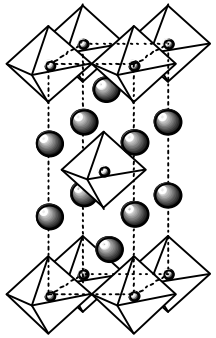

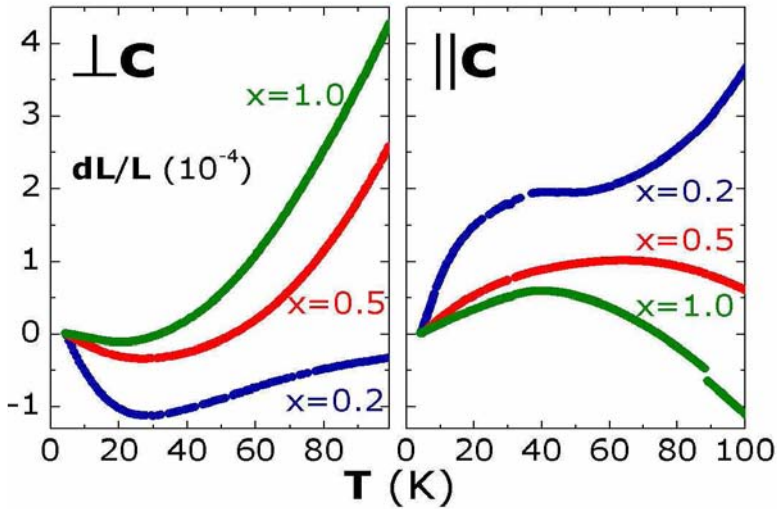

- **low temperature anomaly**
- **strongest for x=0.2**

M. Kriener et al.,
PRL 95, 267403 (2005).

metamagnetism in $Ca_{1.8}Sr_{0.2}RuO_4$

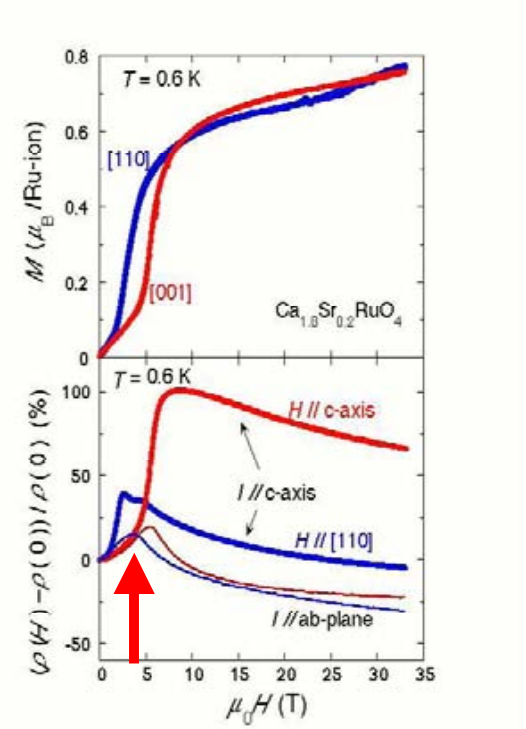

S. Nakatsuji, *et al.*, PRL 2003.

- **field dependencies**

M. Kriener et al.,
PRL 95, 267403 (2005).
J. Baier et al., condmat0610769.

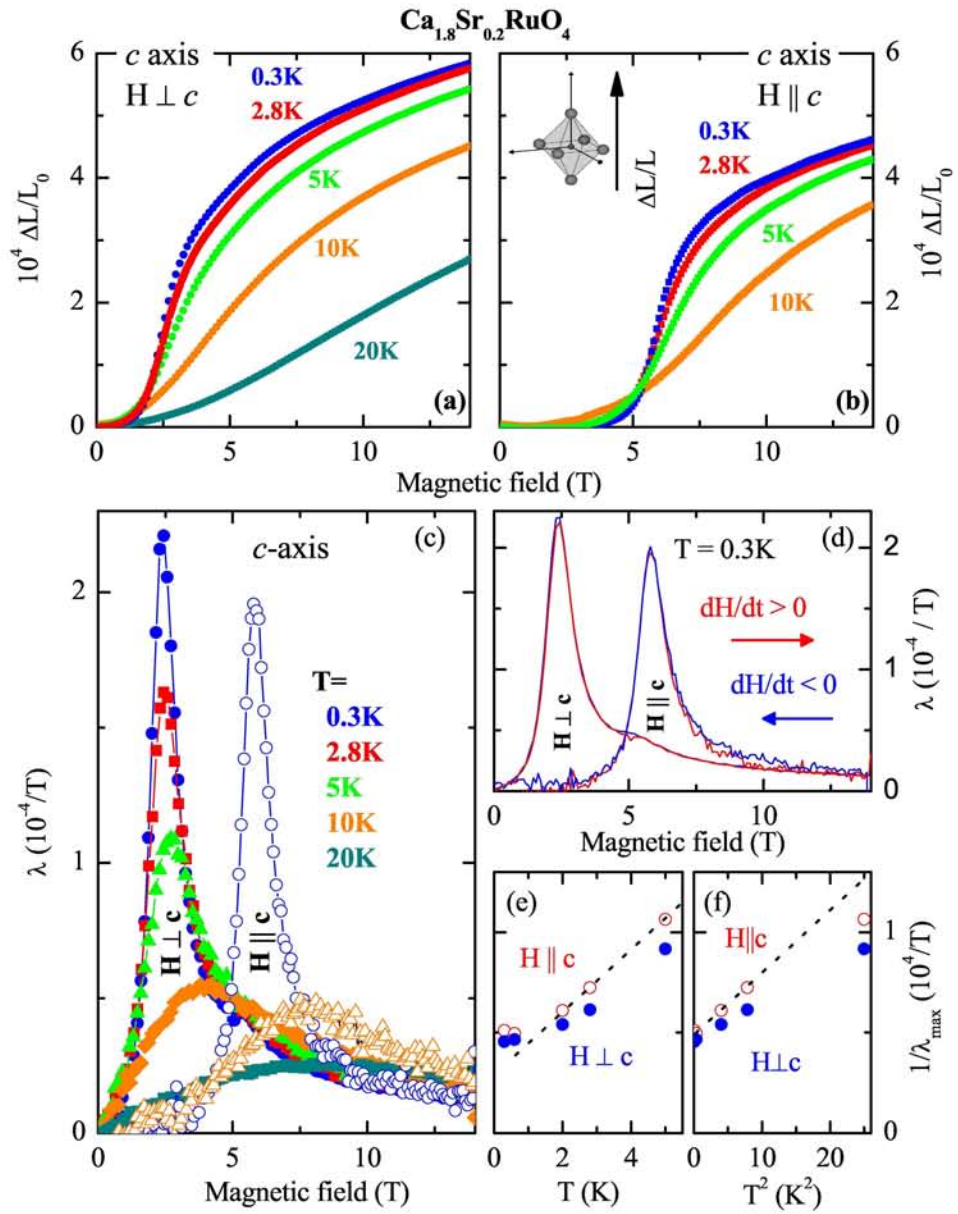

Electronic transition in $Ca_{2-x}Sr_xRuO_4$

neutron-powder-diffraction at high field GEM (ISIS)

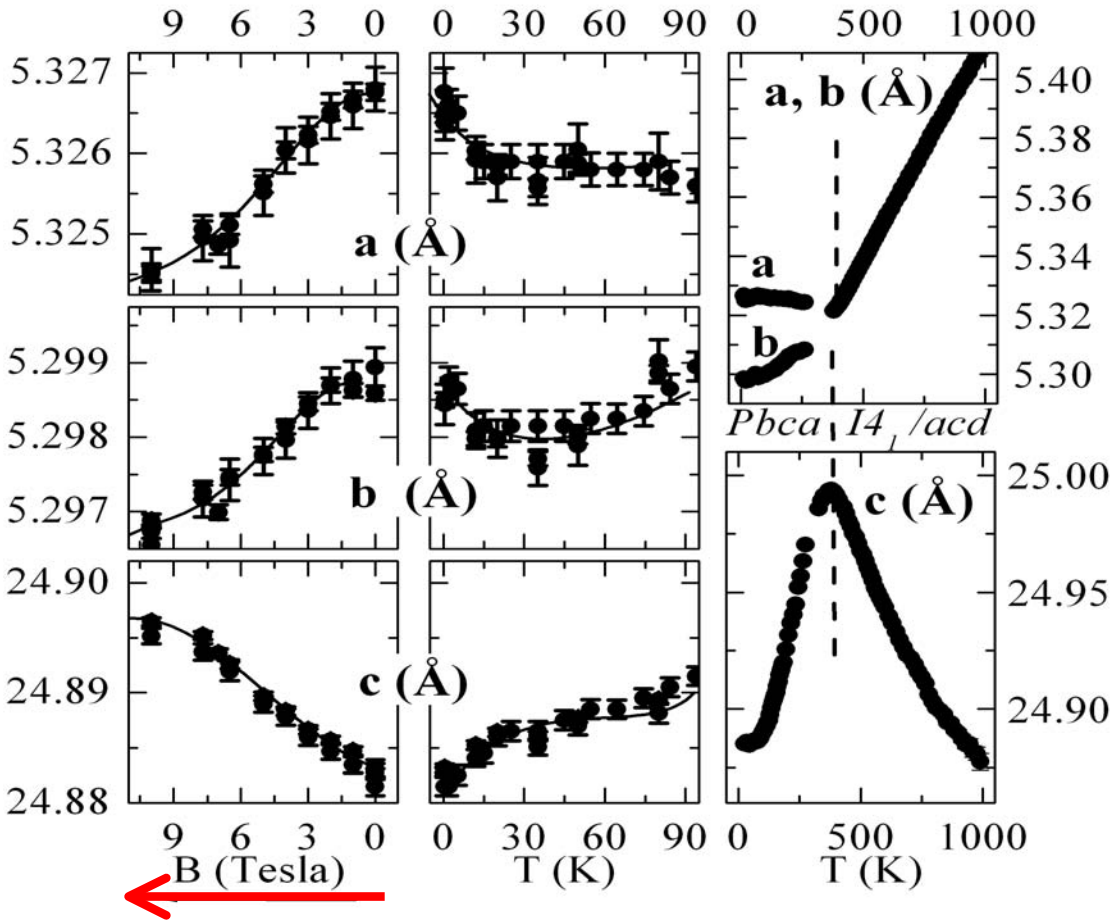

- zero field : lattice flattening
- high field : lattice elongation

Electronic transition in $Ca_{2-x}Sr_xRuO_4$

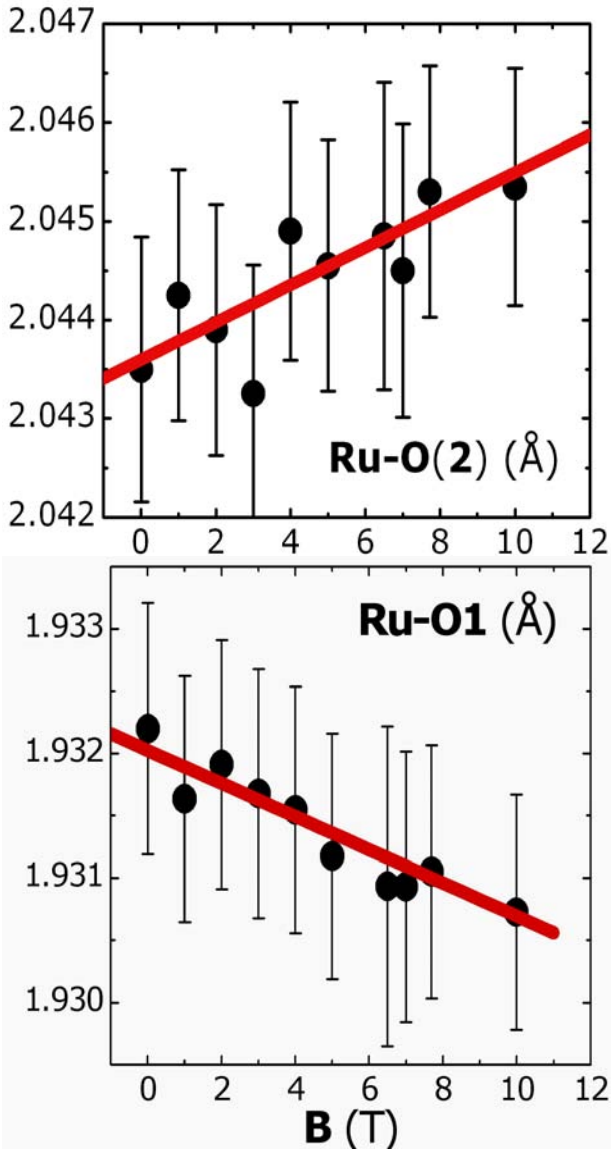

(GEM ISIS & Fullprof)

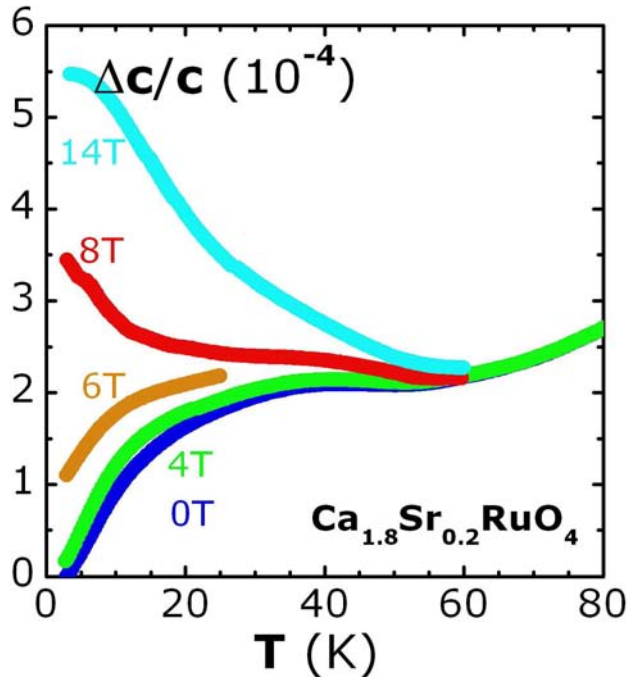

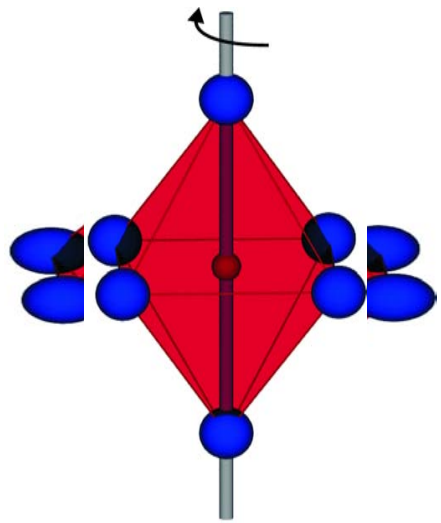

M. Kriener et al.,
PRL 95, 267403 (2005).

- **zero field : octahedron flattening**
- **high field : octahedron elongation**

Tuning of orbital occupation

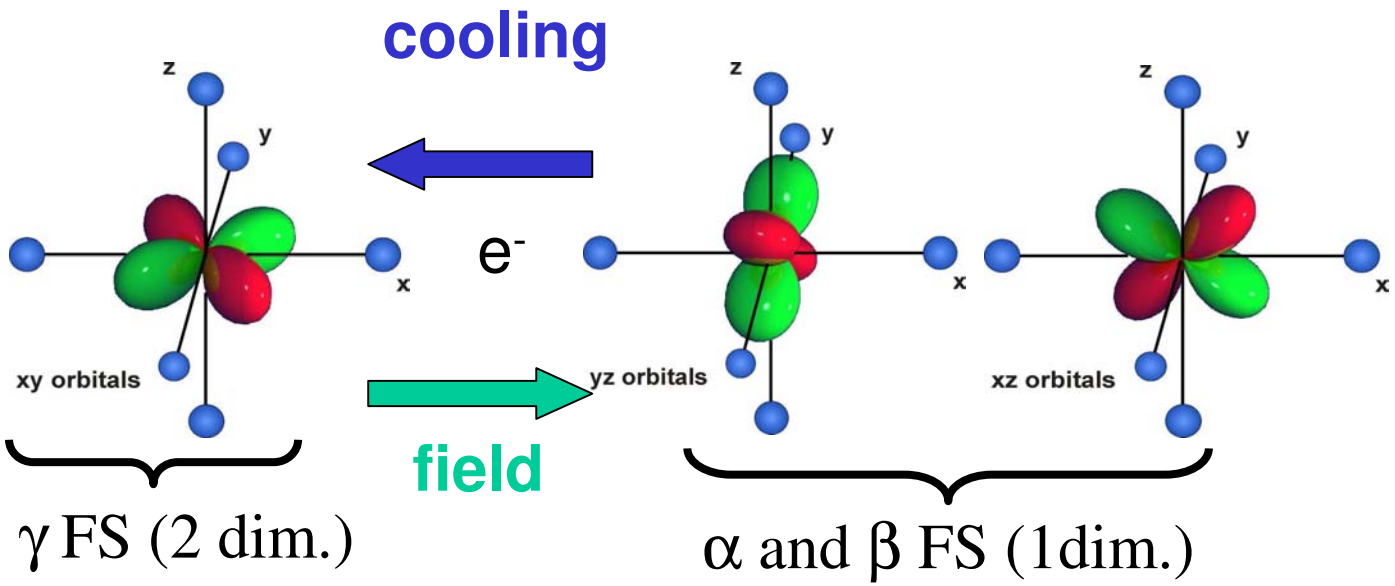

- **nearly localized electrons (close to the Mott transition)**
  ⇒ **high electronic Grüneisen-parameter**

- zero field : electrons move into the γ-band upon cooling
- high field : electrons leave γ-band

strong effects in tilted phase (x~0.2)

Incommensurate scattering around $Ca_{1.5}Sr_{0.5}RuO_4$

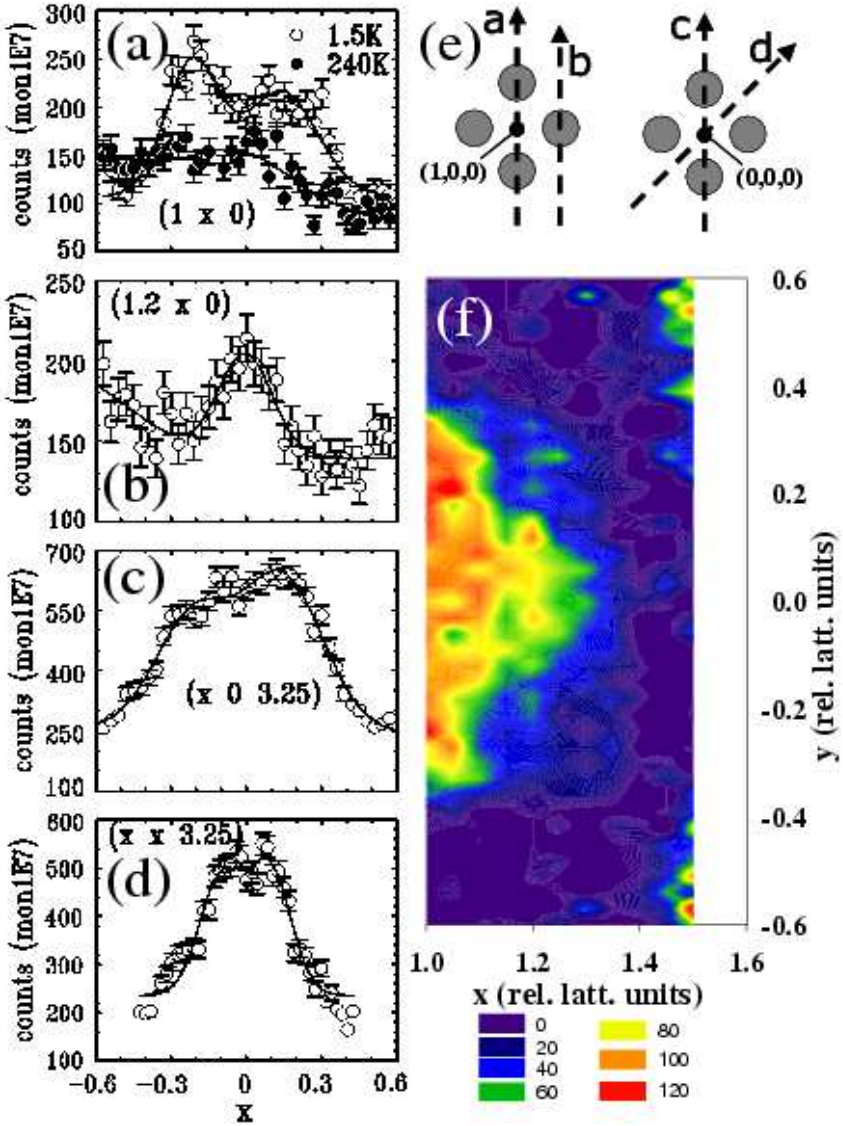

X~0.5

$Ca_{1.38}Sr_{0.62}RuO_4$

scattering near (0.2,0,0)

$$\gamma = \frac{\pi k_B^2}{\hbar} \left\langle \frac{1}{\Gamma(\mathbf{Q})} \right\rangle_{BZ}$$

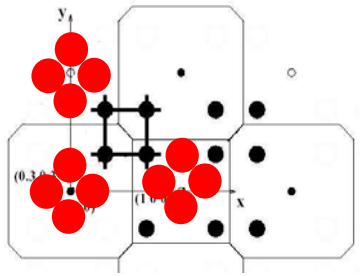

O. Friedt et al., PRL 93, 147404 (2004).

Magnetism of d_{xy}-band

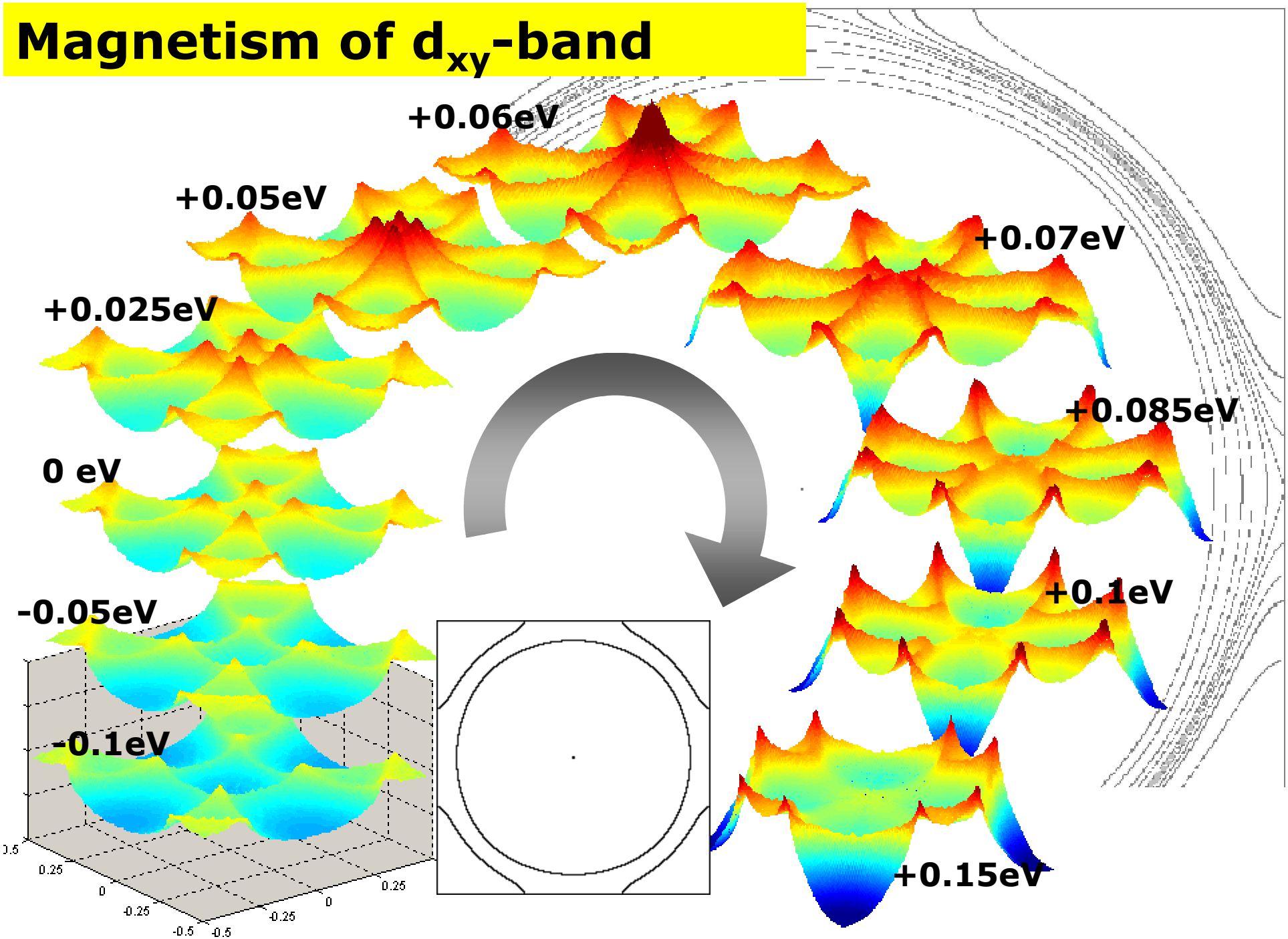

Magnetic fluctuations & metamagnetism

x=0.2 **$Ca_{1.8}Sr_{0.2}RuO_4$**

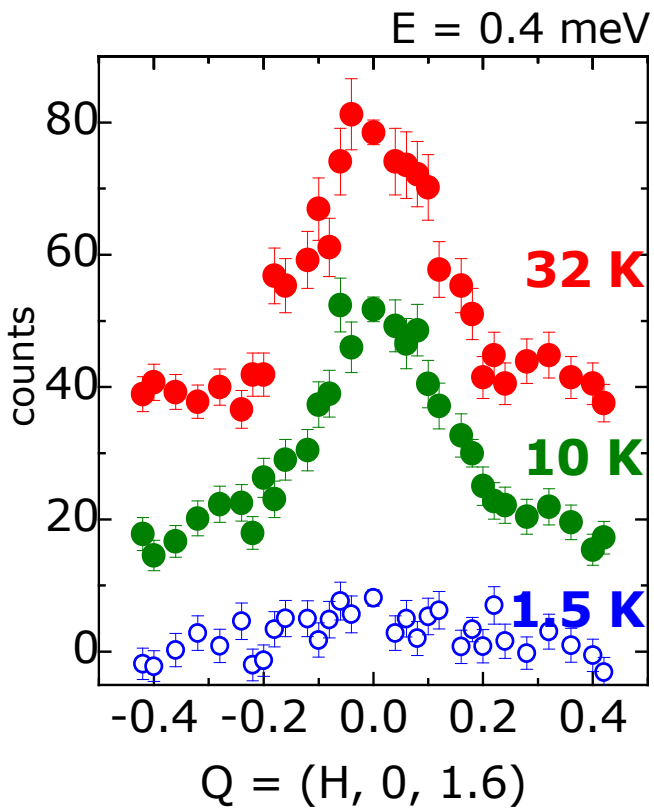

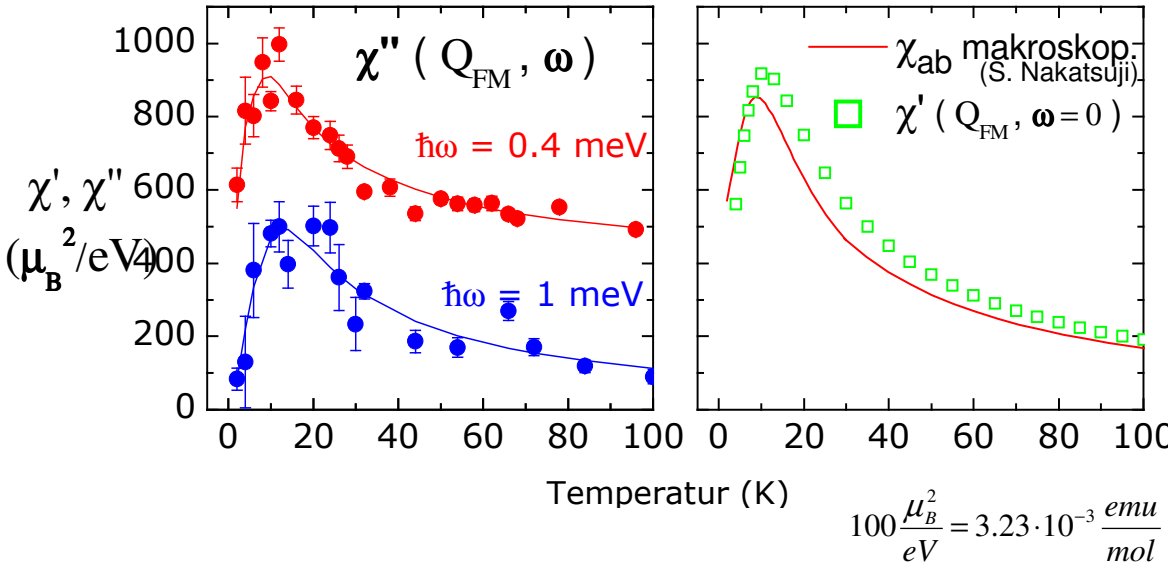

$$\chi''(q,\omega) = \chi'(q,0)\cdot\frac{\Gamma\omega}{\Gamma^2+\omega^2}$$

- **paramagnons** at 10K
- they get suppressed at low T

P. Steffens et al., PRL 2007

$Ca_{1.8}Sr_{0.2}RuO_4$: Magnetic fluctuations

x=0.2

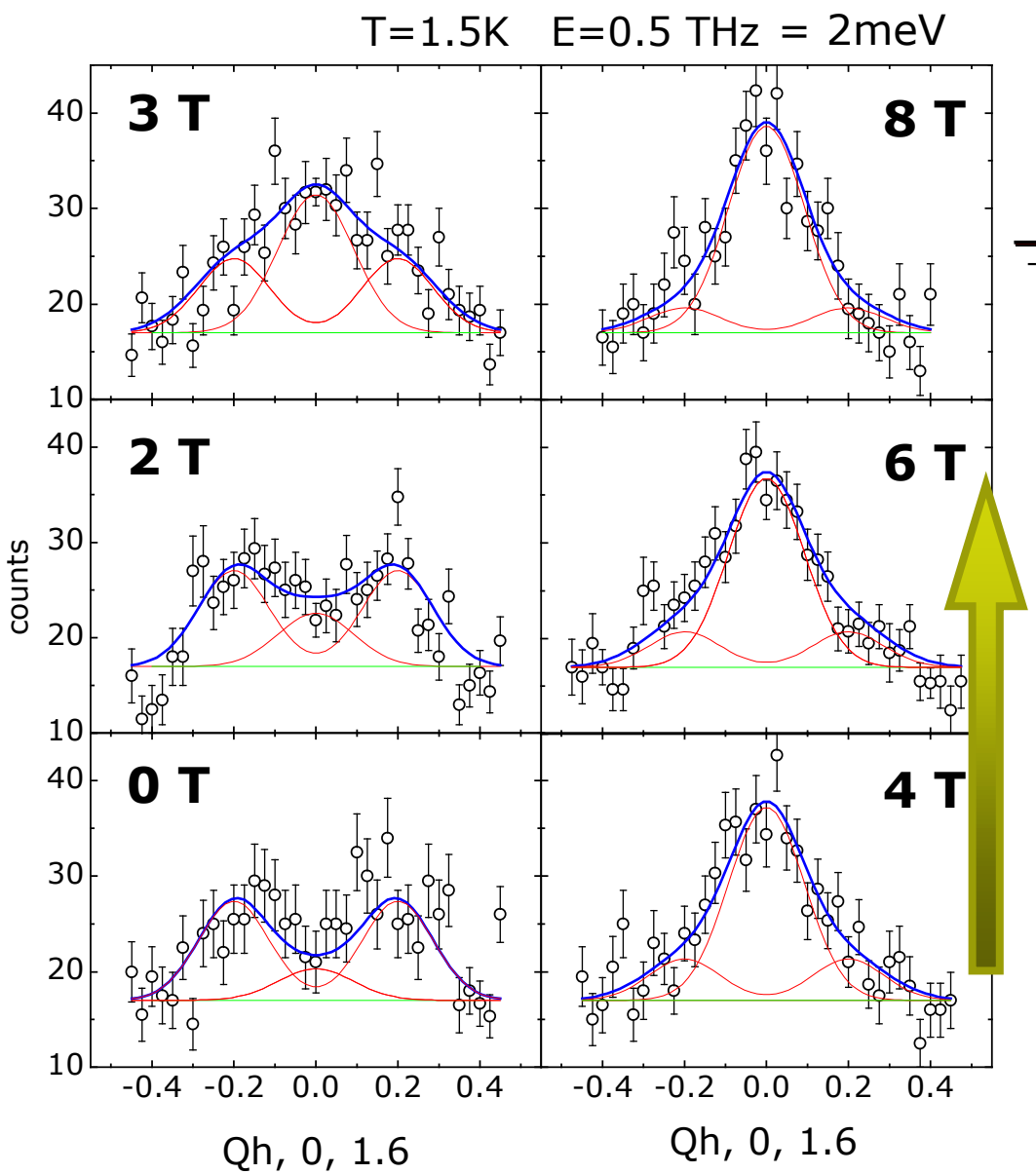

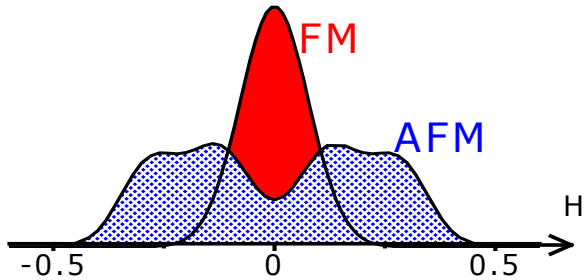

Magnetic field ⇓
FM paramagnons

Magnetic field

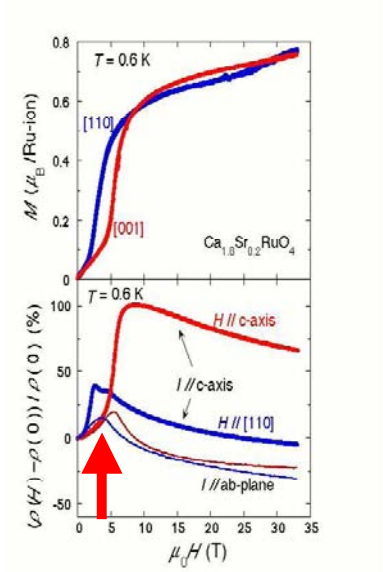

S. Nakatsuji, *et al.*, PRL 2003.

Conclusions

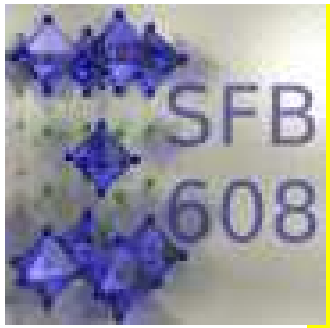

Interplay between charge, orbital and magnetic degrees of freedom in layered-ruthenates.

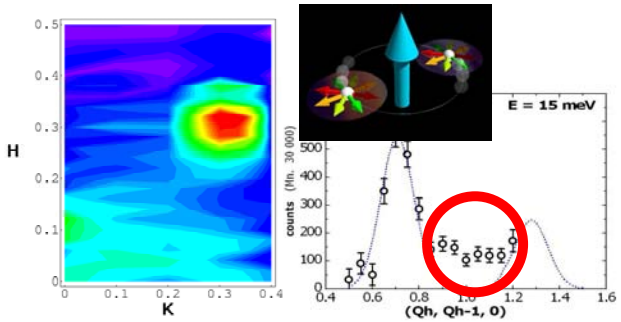

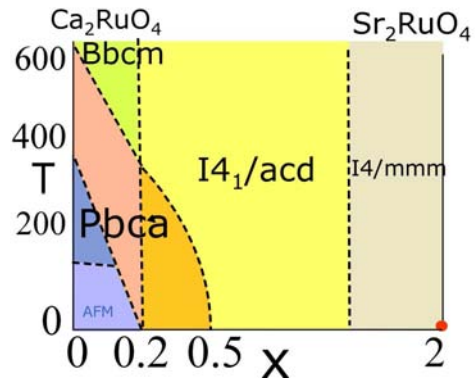

- **pure Sr_2RuO_4 : unconventional superconductor**
  strong nesting-type fluctuations
  but also broad quasi-FM fluctuations

- **metal-insulator transition in Ca_2RuO_4**
  driven through orbital rearrangement
  „continuous“ aspects

- **metamagnetism in $Ca_{2-x}Sr_xRuO_4$**
  very flat bands close to the MI transition (heavy QP)
  orbital occupation important
  competition of at least two magnetic instabilities
  field-induced FM paramagnons